On the Greenhouse Effect

Claude Bardos, Olivier Pironneau

▶ **To cite this version:**

Claude Bardos, Olivier Pironneau. On the Greenhouse Effect. 2021. hal-03094855v4

HAL Id: hal-03094855

https://hal.sorbonne-universite.fr/hal-03094855v4

Preprint submitted on 15 Mar 2021 (v4), last revised 12 May 2021 (v5)

HAL is a multi-disciplinary open access archive for the deposit and dissemination of scientific research documents, whether they are published or not. The documents may come from teaching and research institutions in France or abroad, or from public or private research centers.

L'archive ouverte pluridisciplinaire **HAL**, est destinée au dépôt et à la diffusion de documents scientifiques de niveau recherche, publiés ou non, émanant des établissements d'enseignement et de recherche français ou étrangers, des laboratoires publics ou privés.

On the Greenhouse Effect

Claude Bardos* & Olivier Pironneau†

March 15, 2021

Abstract

Radiative transfer is at the heart of the mechanism to explain the greenhouse effect due to the partial opacity of carbon dioxide, methane and others in the atmosphere. We revisit this much studied field from a mathematical and numerical point of view. Existence and uniqueness and implicit solutions of the Milne problem for grey atmospheres are stated. Numerical simulations are given for grey and non grey atmospheres and applied to the greenhouse effect. In the context of a fully transparent atmosphere for sunlight, it is found that greenhouse gases absorption in the infrared range contributes to a change of temperature of the atmosphere of 2% either by widening the frequency range of infrared absorption and/or augmenting the absorption parameter in the infrared range. On the other hand, the same changes but in the low infrared range of the sunlight leads to a positive change of temperature. Several computer codes were written to validate the results and the range of numbers obtained lead us to think that it is correct but possibly also beyond the precision of the computer programs.

The authors conclude that the radiative transfer model used with an atmosphere transparent to the incident sunlight is not capable of explaining the greenhouse effect due to the so-called GreenHouse Gases increased opacity in the infrared range; a contrario, their absorption rays in the lower frequency range of sunlight could explain the greenhouse effect. Nevertheless, the complexity of a full ocean-atmosphere-biosphere climate model is needed.

Jumping to conclusion on climate change should be cautiously avoided and a review of the hypothesis of the radiative transfer argument commonly found in textbooks should to be preferred.

1 Introduction

The greenhouse effect is an important element of the current theory of climate change. Some gases in the Earth atmosphere like carbon dioxide $\mathtt{CO}_2$ and methane $\mathtt{CH}_4$ absorb infrared rays and thus contribute to a global warming of our planet. As explained in [20],[23],[9] and [13] the Sun radiates light with a heat flux $Q = 1370\text{Watt/m}^2$, in the frequency range $(0.5, 20) \times 10^{14}$ corresponding approximately to a black body at temperature of 5800K; 74% of this light intensity reaches the ground because the atmosphere is almost transparent to this spectrum and about 36% is reflected back by the clouds or the ocean, snow, etc. (albedo).

The Earth behaves almost like a black body at temperature $T_e = 288K$ and as such radiates rays of frequencies ν in the infrared spectrum $(0.03, 0.6) \times 10^{14}$.

So both the Sun and the Earth are approximate black bodies. The Planck theory says that a black body at temperature T radiates electromagnetic waves in the entire frequency spectrum $\nu \in \mathbb{R}^+$ with intensities given by the Planck function:

$$\nu \in \mathbb{R}^+ \mapsto B_\nu(T) = \frac{2\hbar\nu^3}{c^2\left[\mathrm{e}^{\frac{\hbar\nu}{kT}} - 1\right]} \tag{1}$$

where $\hbar$ is the Planck constant, c is the speed of light in the medium and k is the Boltzmann constant.

claude.bardos@gmail.fr, LJLL, Université de Paris, France.

†*olivier.pironneau@sorbonne-universite.fr*, LJLL, Sorbonne Université, Paris, France.

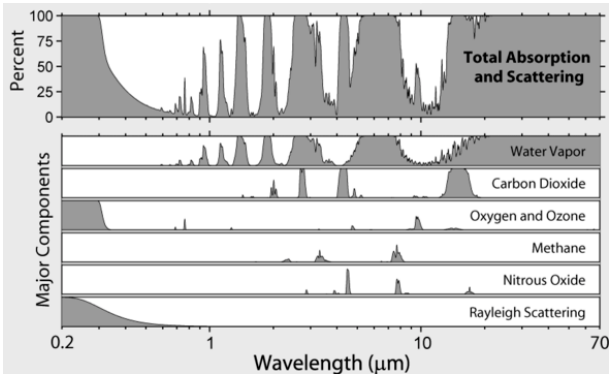

Figure 1: *Absorption coefficient κ_ν of some gases of the atmosphere in the range of frequencies of interest, but versus wave length (c/ν, c being the speed of light). (reprinted from wikipedia). Adding more CO_2 increases κ_ν in the range (8,15)μm.*

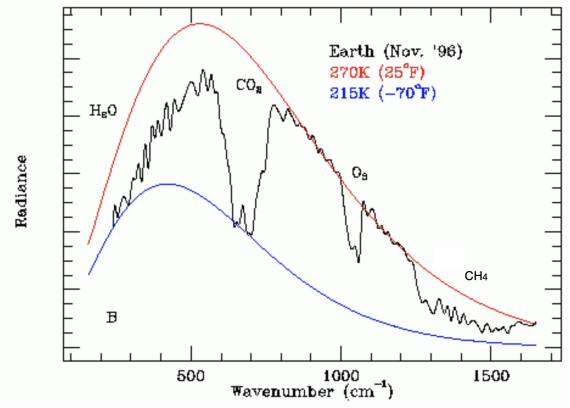

Figure 2: *The thermal infrared emission spectrum of the Sahara, as recorded from deep space by the Mars Global Surveyor (MGS) Spacecraft in November 1996, (reprinted from xylenepower.com). CO_2, O_3, CH_4 are clearly responsible for infrared absorption.*

A major discrepancy between reality and the black body theory for Earth is shown on fig 2. It is due to the partial transparency of the atmosphere and the absorbing power of CO_2, H_2O, O_3, CH_4, etc., in the infrared range. Figure 1 gives the absorption coefficients κ_ν for some gas (a transparent gas has $\kappa_\nu = 0$, and 1 if it is opaque.) Consequently, the infrared light emitted by Earth, seen from far, has a defect of energy in its spectrum which is affected by the proportion of Green-House Gases (GHG): it is the *greenhouse effect*.

In this article we propose a mathematical and numerical investigation to quantify this phenomenon.

Photons travel at the speed of light; energy balance can thus be assumed instantaneous. The atmosphere is affected by wind, rain, chemistry, etc., but at a very different time-scale; it is believed – and to some extent argumented, (see [13]) – that even if all these other phenomena are ignored, still the greenhouse effect is sufficient to explain, partially, global warming. Consequently, in the article, we restrict the analyses to the energy conservation equations for the radiative intensity and the temperature, equations (2) and (3) below.

Radiative transfers have been studied by astronomers and nuclear physicists. Their work is summarized in [8] and [24]. Mathematical analyses are also numerous and we send the readers to [11],[14] and [29].

More recently, for obvious reasons, there is a renewed interest in numerical simulations of radiative transfers. Among others the reader is sent to [17],[16],[10],[21],[19]. However, we are not aware of a simulation of the very specific greenhouse gases (GHG) effect, as presented here.

2 The fundamental equations

Let $I_\nu(\mathbf{x}, \boldsymbol{\omega})$ be the intensity of the radiation of frequency ν in the direction $\boldsymbol{\omega}$ at point $\mathbf{x}$ of the physical domain Ω. Let $T(\mathbf{x})$ be the temperature. Energy balance (see [24],[13]) yields,

$$\boldsymbol{\omega} \cdot \nabla I_\nu + \rho\kappa_\nu a_\nu \left[I_\nu - \frac{1}{4\pi} \int_{\mathbb{S}^2} p(\boldsymbol{\omega}, \boldsymbol{\omega}') I_\nu(\boldsymbol{\omega}') \mathrm{d}\omega' \right] = \rho\kappa_\nu (1 - a_\nu)[B_\nu(T) - I_\nu], \tag{2}$$

$$-\kappa_T \Delta T = \nabla \cdot \int_0^\infty \frac{1}{4\pi} \int_{\mathbb{S}^2} I_\nu(\boldsymbol{\omega}') \boldsymbol{\omega}' \mathrm{d}\omega' \mathrm{d}\nu. \tag{3}$$

Here, $\mathbb{S}^2$ is the unit sphere, $\rho(\mathbf{x})$ is the density of the medium, κ_ν is the absorption coefficient (percentage absorbed per unit length), a_ν is the scattering coefficient; $\frac{1}{4\pi} p(\boldsymbol{\omega}, \boldsymbol{\omega}')$ is the probability that a ray in the direction $\boldsymbol{\omega}$ scatter in the direction $\boldsymbol{\omega}'$, (recall that $\frac{1}{4\pi} \int_{\mathbb{S}^2} p(\boldsymbol{\omega}, \boldsymbol{\omega}') \mathrm{d}\omega' = 1$); both κ_ν and a_ν usually depend on ν, and even $\mathbf{x}$. The constant κ_T is the thermal diffusion.

As usual, boundary conditions have to be given. For the temperature we may prescribe its normal derivative to be zero for all $\mathbf{x} \in \partial\Omega$. The equation for the intensity being a first order equation, I_ν should be given on Σ^- defined as

$$\Sigma_- = \{(\mathbf{x}, \boldsymbol{\omega}) \in \partial\Omega \times \mathbb{S}^2 : \quad \mathbf{n}(\mathbf{x}) \cdot \boldsymbol{\omega} < 0\}, \tag{4}$$

where $\mathbf{n}$ is the outer unit normal of $\partial\Omega$. However, we will deal also with cases which use on Σ_- some of the information arriving on $\Sigma_+ = \{(\mathbf{x}, \boldsymbol{\omega}) \in \partial\Omega \times \mathbb{S}^2 : \quad \mathbf{n}(\mathbf{x}) \cdot \boldsymbol{\omega} > 0\}$.

2.1 Isotropic scattering

Proposition 1

$$\nabla \cdot \int_{\mathbb{S}^2} I_\nu(\boldsymbol{\omega}) \boldsymbol{\omega} \, d\omega = \rho\kappa_\nu(1 - a_\nu) \left(4\pi B_\nu(T) - \int_{\mathbb{S}^2} I_\nu(\boldsymbol{\omega}) \, d\omega\right). \tag{5}$$

Proof. It is shown by averaging (2) on $\mathbb{S}^2$.

Corollary 1 *The temperature equation which is normally written with a flux of radiative energy (3), can also be recast as (6):*

$$-\kappa_T \Delta T - \int_0^\infty \rho\kappa_\nu(1 - a_\nu) \left(B_\nu(T) - \frac{1}{4\pi} \int_{\mathbb{S}^2} I_\nu(\boldsymbol{\omega}) \, d\omega\right) d\nu = 0. \tag{6}$$

Corollary 2 *If the thermal diffusion κ_T is neglected in (6), then*

$$\int_0^\infty \kappa_\nu(1 - a_\nu) B_\nu \, d\nu = \int_0^\infty \kappa_\nu(1 - a_\nu) \frac{1}{4\pi} \int_{\mathbb{S}^2} I_\nu(\boldsymbol{\omega}) \, d\omega \, d\nu. \tag{7}$$

Remark 1 *When κ_ν and a_ν are constant, (7) leads to the Stefan-Boltzmann law*

$$\sigma_b T^4 = \int_0^\infty \frac{1}{4\pi} \int_{\mathbb{S}^2} I_\nu(\boldsymbol{\omega}) \, d\omega d\nu, \ \text{with } \sigma_b = \frac{2\hbar}{15c^2} \left(\frac{k\pi}{\hbar}\right)^4. \tag{8}$$

Note that the standard definition of the Stefan-Boltzmann constant has an extra π.

Some proofs concerning the existence, uniqueness and stability for solutions of simplified versions of this problem appear below. The most general case is discussed in the conclusion with relevant and updated references.

3 One dimensional approximations

Proposition 2 *Consider (2),(7) in a vertical slab $\Omega = (0, H) \times \mathbb{R}^2$. Assume that the boundary conditions at $\mathbf{x} = (x, y, z)$ are independent of y, z, and assume isotropic scattering ($p \equiv 4\pi$). Let $\mathbf{n}$ be the outer unit normal at $z = H$. Then, the solution depends only on x and $\mu = \cos\phi = \boldsymbol{\omega} \cdot \mathbf{n}$ and $I_\nu(\mathbf{x}, \boldsymbol{\omega}) = I'_\nu(x, \mu)$ and $T(x)$ are given by (1) and*

$$\mu \partial_x I'_\nu + \rho\kappa_\nu a_\nu \left(I'_\nu - \frac{1}{2} \int_{-1}^1 I'_\nu(x, \mu) d\mu\right) + \rho\kappa_\nu(1 - a_\nu)[I'_\nu - B_\nu] = 0, \quad \text{for all } x \in (0, H), \ \mu \in (-1, 1), \tag{9}$$

$$\int_0^\infty \kappa_\nu(1 - a_\nu) B_\nu \, d\nu = \int_0^\infty \left(\kappa_\nu(1 - a_\nu) \frac{1}{2} \int_{-1}^1 I_\nu(x, \mu) \, d\mu\right) d\nu, \quad \text{for all } x \in (0, H). \tag{10}$$

Proof : Assume that B_ν is a given function of x only. Both problems (2) and (9) have one and only one solution. Let us show that $I_\nu(x, y, z, \omega_1, \omega_2, \omega_3) = I'_\nu(x, \cos\phi)$ is a solution of (2) when I'_ν is a solution of (9).

Let $\mathbf{t}$ be the direction of the projection $\boldsymbol{\omega}_t$ of $\boldsymbol{\omega}$ on the plane P of the slab boundary. I_ν is invariant in $\mathbf{t}$. Hence $\boldsymbol{\omega}_t = \{\omega_1, \omega_2\} = \{\cos\phi, \sin\phi\}^T$,

$$\boldsymbol{\omega} \cdot \nabla I_\nu = \omega_1 \partial_x I_\nu + \omega_2 \partial_t I_\nu = \cos\phi \partial_x I'_\nu + \sin\phi \partial_t I'_\nu = \cos\phi \partial_x I'_\nu + 0 = \mu \partial_x I'_\nu.$$

$$\frac{1}{4\pi}\int_{\mathbb{S}^2} I_\nu(x,\mu)\mathrm{d}\omega = \frac{1}{4\pi}\int_0^{2\pi}\int_{-\pi}^{\pi} I'_\nu(x,\cos\phi)(-\sin\phi)d\phi d\psi = \frac{1}{2}\int_{-1}^{1} I'_\nu(x,\mu)d\mu.$$

Once $I_\nu(x,\mu)$ known, then B_ν becomes a function of x only by (7). □

3.1 Application to the Earth-Sun problem

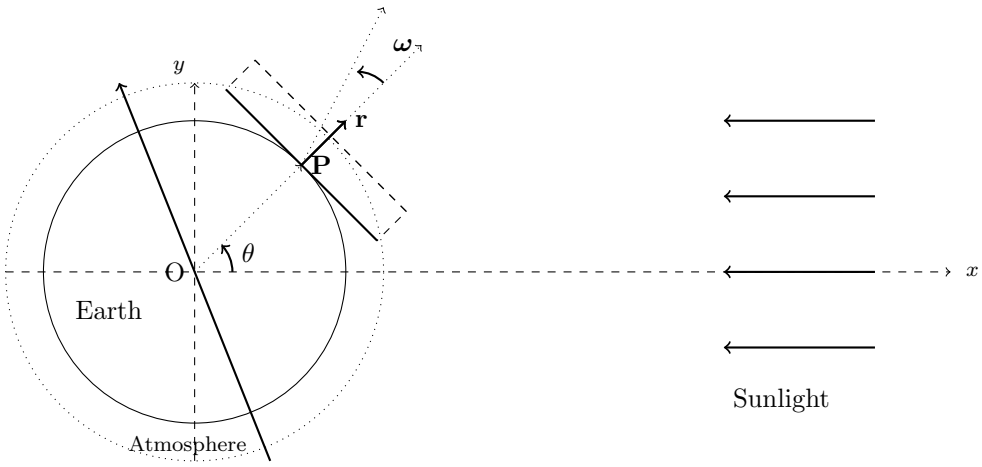

Figure 3: *The Sun, in the far right, sends sunlight to point P on the Earth surface. A crossection of Earth and its atmosphere is shown in the plane defined by the axis Ox and the point P. The projection of the Earth rotation axis in that plane is shown (bold line) but plays no role. As the Earth radius R is large compared with the atmosphere thickness H we focus on a rectangle tangent to the Earth surface at P. In the end the radiative transfer equations are set on the line (P,r), function of the angle $\boldsymbol{\omega}$ where radiation intensity is observed.*

Consider figure 3 and apply the invariance of Proposition 2 to the rectangle tangent to Earth at point P on its surface. The rectangle has width H, the thickness of the atmosphere and length L small compared to the Earth radius R.

Accordingly I' depends only on the radial distance r to P, $r \in (0,H)$ andof μ, the cosine of angle of the ray from $P\mathbf{r}$ to the observer. So $I'(r,\mu)$ is studied for $r \in (0,H)$ and $\mu \in (-1,1)$.

If sunlight hits the tangent plane to Earth at P at a constant angle θ with a frequency dependent intensity Q_ν and if the atmosphere is transparent at that frequency, then

$$I'_\nu(0,\mu) = \mu Q_\nu \cos\theta, \forall \mu \in (0,1), \quad I'_\nu(H,\mu) = 0, \forall \mu \in (-1,0). \tag{11}$$

The first condition applies only when $\mu > 0$ because $\mu < 0$ corresponds to the backside of the tangent plane. In the black body approximation of the Sun, $Q_\nu = Q\nu^3/(\mathrm{e}^{\frac{\nu}{T_{Sun}}} - 1)$ with Q constant.

The second condition says that at the top of the atmosphere no rays come back into the atmosphere.

Now I' is uniquely defined by (9)(10)(11) and it is proportional to $Q\cos\theta$. Hence to compute T at all points of planet Earth, one needs only to compute it at the point of intersection of the sphere and the Sun-Earth line and then multiply by $\cos\theta$. Reality is definitely more complex because this theory implies, in particular, that the Earth temperature at night is zero Kelvin!

Note In this article we focus on methods rather than numbers; for clarity we neglect the scattering, i.e. $a_\nu = 0$, however, much of what is derived below applies also when isotropic scattering is present.

3.2 Spherical symmetry

Chandrasekhar showed in [8] that the one dimensionality argument of Proposition 2, using a tangent plane to Earth, can be extended to planets by using an osculatory spherical cap instead of a tangent plane, to take into account the radius of the planet.

For clarity, consider a spherical planet receiving parallel light rays from infinity. The planet's radius is R and its atmosphere thickness is H. Let the radial distance to the surface be $r = |\mathbf{x}| - R$. Invariance with respect to the azimuthal and latitude angles, after suitable scalings by the appropriate cosines, and a similar argument as above, lead to the Chandrasekhar correction (see [8]):

$$\mu \frac{\partial \bar{I}_\nu}{\partial r} + \frac{1-\mu^2}{R+r}\frac{\partial \bar{I}_\nu}{\partial \mu} + \kappa_\nu \rho \left(\bar{I}_\nu - B_\nu(T)\right) = 0, \quad \forall r, \mu, \nu \in (0,H)\times(-1,1)\times\mathbb{R}^+. \tag{12}$$

and if thermal diffusion is neglected:

$$\int_0^\infty \rho\kappa_\nu \left(B_\nu(T) - \frac{1}{2}\int_{-1}^1 \bar{I}_\nu \mathrm{d}\mu\right) d\nu = 0, \quad \forall r \in (0,H). \tag{13}$$

Note that no additional boundary condition to (11) is needed because $1-\mu^2$ is zero at $\mu = \pm 1$.

3.3 Dimensionless variables

These "Chandrasekhar equations" can be adimentionalised by introducing a length scale λ, scaling factors for B, ν and ρ and set: $r = \tilde{r}\lambda$, $R = \tilde{R}\lambda$ and $H = \tilde{H}\lambda$, $\rho = \rho_0\tilde{\rho}$, $\nu = \nu_0\tilde{\nu}$ and $B = B_0\tilde{B}$. Then we may rewrite the above and its boundary conditions as :

$$\begin{aligned} &\mu \frac{\partial \tilde{I}_{\tilde{\nu}}}{\partial \tilde{r}} + \frac{1-\mu^2}{\tilde{R}+\tilde{r}}\frac{\partial \tilde{I}_{\tilde{\nu}}}{\partial \mu} + \tilde{\kappa}_{\tilde{\nu}}\tilde{\rho}\left(\tilde{I}_{\tilde{\nu}} - \tilde{B}_{\tilde{\nu}}(\tilde{T})\right) = 0, \quad \int_0^\infty \tilde{\kappa}_{\tilde{\nu}}\left(\tilde{B}_{\tilde{\nu}}(\tilde{T}) - \frac{1}{2}\int_{-1}^1 \tilde{I}_{\tilde{\nu}}\mathrm{d}\mu\right)\mathrm{d}\tilde{\nu} = 0, \\ &\tilde{I}_{\tilde{\nu}}(H,\mu) = 0, \forall \mu \in (-1,0), \quad \tilde{I}_{\tilde{\nu}}(0,\mu) = \mu B_0^{-1} Q_{\tilde{\nu}} \cos\theta, \forall \mu \in (0,1) \end{aligned} \tag{14}$$

with

$$\tilde{\kappa}_{\tilde{\nu}} = \lambda\rho_0\kappa_\nu, \ \tilde{B} = B_0^{-1}\frac{2h\nu_0^3}{c^2}\frac{\tilde{\nu}^3}{\mathrm{e}^{\frac{\tilde{\nu}}{\tilde{T}}}-1}, \ T = \frac{\hbar\nu_0}{k}\tilde{T}, \ \bar{I}_{\tilde{\nu}} = B_0\tilde{I}_{\tilde{\nu}}. \tag{15}$$

3.4 Evanescent atmosphere

When $\rho = \rho_0 \mathrm{e}^{-\tilde{r}}$, we make a last change of variable (analogous to the optical depth introduced in physics) to cope with that exponentially rarefying atmosphere: $(r,\mu) \to (\tau := 1 - \mathrm{e}^{-\tilde{r}}, \mu)$. Then, with $Z = 1 - \mathrm{e}^{-\tilde{H}}$, for all $\tau, \mu, \nu \in (0,Z)\times(-1,1)\times\mathbb{R}^+$,

$$\begin{aligned} &\mu\frac{\partial \tilde{I}_\nu}{\partial \tau} + \gamma(\tau,\mu)\frac{\partial \tilde{I}_\nu}{\partial \mu} + \tilde{\kappa}_\nu\left(\tilde{I}_\nu - \tilde{B}_\nu\right) = 0, \quad \int_0^\infty \tilde{\kappa}_\nu\left(\tilde{B}_\nu(T) - \frac{1}{2}\int_{-1}^1 \bar{I}_\nu \mathrm{d}\mu\right)d\tilde{\nu} = 0. \\ &\tilde{I}_\nu(Z,\mu) = 0, \forall \mu \in (-1,0), \quad \tilde{I}_\nu(0,\mu) = \mu\tilde{Q}_\nu, \forall \mu \in (0,1), \end{aligned} \tag{16}$$

where $\tilde{Q}_\nu = Q_\nu \cos\theta / B_0$. The Chandrasekhar correction is

$$\gamma(\tau,\mu) = \frac{1-\mu^2}{(1-\tau)(\tilde{R} - \log(1-\tau))} \tag{17}$$

Remark 2 *For clarity, from now on, we drop the tildes.*

3.5 Grey atmosphere

By definition, in a grey atmosphere (Fowler [13] p70), nothing depends on ν. If in addition the thermal diffusion is neglected, i.e. $\kappa_T = 0$, then the total radiation, $I = \int_0^\infty I_\nu d\nu$, is given by (11) integrated in ν, and

$$\mu \frac{\partial I}{\partial \tau} + \gamma \partial_\mu I = \kappa[B - I] \text{ with } B(\tau) = \int_0^\infty B_\nu(T) d\nu = \frac{1}{2} \int_{-1}^{1} I \mathrm{d}\mu. \tag{18}$$

Temperature is recovered from $B(\tau) = \sigma_b T^4(\tau)$.

3.6 The multi-groups problem

In numerical computations one replaces the continuous map $\nu \mapsto I_\nu$ by a finite set of frequencies $\{\nu_k, I_k\}_1^K$, and write the system

$$\begin{aligned} &\mu \frac{\partial I_k}{\partial \tau} + \gamma(\tau, \mu) \frac{\partial I_k}{\partial \mu} + \kappa_{\nu_k} (I_k - B_{\nu_k}(T)) = 0, \quad \sum_k \kappa_{\nu_k} \left(B_{\nu_k}(T) - \frac{1}{2} \int_{-1}^{1} I_k \mathrm{d}\mu \right) (\nu_k - \nu_{k-1}) = 0, \\ &I_k(Z, \mu)|_{\mu<0} = 0, \quad I_k(0, \mu)|_{\mu>0} = \mu Q_{\nu_k}, \quad k = 1, \ldots, K. \end{aligned} \tag{19}$$

Recall that $T = \{T_k\}$, which is a function of τ only, couples all the $\{I_k\}$. This formulation will be used in the numerical section 7.

3.7 The Milne problem

When γ is neglected in (18), the problem is known as Milne's problem in $\Omega = (0, Z) \times (-1, 1)$:

$$\mu \frac{\partial I}{\partial \tau} + \kappa \left(I - \frac{1}{2} \int_{-1}^{1} I \mathrm{d}\mu \right) = 0, \ \forall \tau, \mu \in \Omega, \quad I(Z, \mu)|_{\mu<0} = 0, \quad I(0, \mu)|_{\mu>0} = \mu. \tag{20}$$

where κ (i.e. $\kappa_\nu \rho_0$) is constant.

4 More about the Milne problem

Emphasis on the Milne problem is motivated by the two following facts.

- It corresponds to a local in space description of the atmosphere say of eight Z because for R large compared to Z the Chandrasekhar correction can be neglected.
- One can introduce the point of view of functional analysis (cf. [11] chapter 21 Vol 9) without going into details but keeping things *as explicit as possible*.
- One can also use very explicit computations which were derived at the time when computers were not available, say in the middle of the previous century.

We consider the abstract problem (22) in $\Omega = (0, Z) \times (-1, 1)$.

Theorem 1 *With*

$$f \in L^2(\Omega) \quad \mu^{\frac{1}{2}} g_0 \in L^2(0, 1) \quad \textit{and} \quad |\mu|^{\frac{1}{2}} g_Z \in L^2(-1, 0) \tag{21}$$

the problem

$$\mu \partial_\tau I + I - \frac{1}{2} \int_{-1}^{1} I(\tau, \mu') d\mu' = f, \ I(0, \mu)|_{\mu>0} = g_0(\mu), \ I(Z, \mu)|_{\mu<0} = g_Z(\mu), \tag{22}$$

has a unique solution $I \in L^2(\Omega))$ which satisfies the estimates:

$$\|I\|_{L^2(\Omega)} \le C(Z) \left\{ \|f\|_{L^2(\Omega)} + \|\mu^{\frac{1}{2}} g_0(\mu)\|_{L^2(0,1))} + \||\mu|^{\frac{1}{2}} g_Z(\mu)\|_{L^2(-1,0))} \right\} \tag{23a}$$

Moreover when the data f, g_0, g_Z are non negative , the same is true for I, the solution of (22). With $f = 0$ one has:

$$\sup I(\tau,\mu) \le \sup\Big(\sup_{\mu\in(0,1)} g_0(\mu),\ \sup_{\mu\in(-1,0)} g_Z(\mu)\Big)\Big). \tag{23b}$$

Proof : The leading ideas are given below while details can be found in ([11]). They are all based on the estimate of physical quantities which are translated into "mathematical" norms. When unambiguous, the symbol $\|.\|$ will be used below to denote, the L^2 norm in $(L^2(\Omega)$, $L^2_\mu(-1,1)$, $L^2_\mu(0,1)$ and $L^2_\mu(-1,0)$; the subscript μ indicates the variable of integration. Observe that the formula,

$$I(\tau,\mu) = \frac{1}{2}\int_{-1}^{1} I(\tau,\mu)d\mu + \Big(I(\tau,\mu) - \frac{1}{2}\int_{-1}^{1} I(\tau,\mu)d\mu\Big), \tag{24}$$

gives the decomposition of $I \in L^2_\mu(-1,1)$ in its orthogonal projection on the space of μ-independent functions and on its orthogonal (i.e. function of 0 μ average).

One introduces for $\epsilon \ge 0$ the regularized equation:

$$\epsilon I_\epsilon + \mu\partial_\tau I_\epsilon + I_\epsilon - \frac{1}{2}\int_{-1}^{1} I_\epsilon(\tau;\mu')d\mu' = f(\tau,\mu)\,,\ I_\epsilon(0,\mu)|_{\mu>0} = g_0(\mu),\ I_\epsilon(Z,\mu)|_{\mu<0} = g_Z(\mu). \tag{25}$$

A priori estimate and uniqueness

Let us multiply this equation by I_ϵ and integrate with respect to τ and μ :

$$\epsilon\int_\Omega I_\epsilon^2 \mathrm{d}\tau\mathrm{d}\mu + \int_{-1}^{1}\frac{\mu}{2}I_\epsilon^2\Big|_0^Z \mathrm{d}\mu + \int_\Omega I_\epsilon\Big(I_\epsilon - \frac{1}{2}\int_{-1}^{1} I_\epsilon \mathrm{d}\mu\Big)\mathrm{d}\tau\mathrm{d}\mu = \int_\Omega I_\epsilon f \mathrm{d}\tau\mathrm{d}\mu. \tag{26}$$

Notice that

$$\int_\Omega I_\epsilon\Big(I_\epsilon - \frac{1}{2}\int_{-1}^{1} I_\epsilon \mathrm{d}\mu\Big)\mathrm{d}\tau\mathrm{d}\mu = \int_\Omega \Big|I_\epsilon - \frac{1}{2}\int_{-1}^{1} I_\epsilon \mathrm{d}\mu\Big|^2 \mathrm{d}\tau\mathrm{d}\mu.$$

Hence

$$\|I_\epsilon\|^2_{L^2(\Omega)} + \|I_\epsilon - \frac{1}{2}\int_{-1}^{1} I_\epsilon(\tau,\mu)d\mu\|^2_{L^2(\Omega)} + \int_{\Sigma_+}\frac{|\mu|}{2}I_\epsilon^2\mathrm{d}\mu = \int_{\Sigma_-}\frac{|\mu|}{2}I_\epsilon^2\mathrm{d}\mu + \int_\Omega I_\epsilon f\mathrm{d}\tau\mathrm{d}\mu; \tag{27}$$

using the Cauchy Schwartz inequality:

$$\epsilon\|I_\epsilon\|^2_{L^2(\Omega)} + \|I_\epsilon - \frac{1}{2}\int_{-1}^{1} I_\epsilon(\tau,\mu)d\mu\|^2_{L^2(\Omega)} \le \|I_\epsilon\|_{L^2(\Omega)}\|f\|_{L^2(\Omega)} + \||\mu|^{\frac{1}{2}}I_\epsilon\|_{L^2(\Sigma_-)}\||\mu|^{\frac{1}{2}}g(\tau,\mu)\|_{L^2(\Sigma_-)}\,. \tag{28}$$

Since the problem is linear, denoting by $I^1_\epsilon - I^2_\epsilon$ the difference of two solutions with the same boundary data g_0 and g_Z and same external density f , one deduces from (28) the uniqueness because

$$\epsilon\|I^1_\epsilon - I^2_\epsilon\|^2_{L^2(\Omega)} + \|I^1_\epsilon - I^2_\epsilon - \frac{1}{2}\int_{-1}^{1}(I^1_\epsilon - I^2_\epsilon)\mathrm{d}\mu\|^2_{L^2(\Omega)} \le 0. \tag{29}$$

To extend this observation to the case $\epsilon = 0$ one observes that in such case (29) gives:

$$\|I^1_\epsilon - I^2_\epsilon - \frac{1}{2}\int_{-1}^{1}(I^1_\epsilon - I^2_\epsilon)\mathrm{d}\mu\|^2_{L^2(\Omega)} = 0 \tag{30}$$

which gives the relation

$$\mu\partial_\tau(I^1 - I^2) = 0\,,\ \text{with } I^j(0,\mu) = 0 \text{ for } \mu > 0\,,\ \text{and with } I^j(Z,\mu) = 0 \text{ for } \mu < 0, j = 1,2, \tag{31}$$

which implies $I^1 = I^2$.

◇

Existence of Solutions for $\epsilon > 0$

For clarity the proof of the estimate (28) and of the existence of a solution I_ϵ are done in the absence of boundary source. Then, using the linearity of the problem it can be easily adapted to more general situations. First with $\epsilon > 0$ for (28) one obtains a trivial stability estimate

$$\|\tilde{I}_\epsilon\|^2_{L^2(\Omega)} \leq \frac{1}{\epsilon}\|f\|^2_{L^2(\Omega)} \tag{32}$$

To prove the existence of the solution one considers with $\epsilon > 0$ the Milne problem (22) in an iterative form,

$$(1+\epsilon)I^{n+1}_\epsilon + \mu\partial_\tau I^{n+1}_\epsilon = \frac{1}{2}\int_{-1}^{1} I^n_\epsilon(\tau;\mu)d\mu + f(\tau,\mu), \tag{33}$$

leading to the estimate

$$\|I^{n+1}_\epsilon\| \leq \frac{1}{1+\epsilon}(\|I^n_\epsilon\| + \|f\|), \tag{34}$$

which shows that the mapping $I^n_\epsilon \mapsto I^{n+1}_\epsilon$ is a strict contraction.

Then the same type of proof works also for the case $f = 0$ with non zero incoming data on Σ_- with the estimate:

$$\|I^{n+1}_\epsilon\|^2 \leq \frac{1}{1+\epsilon}(\|I^n_\epsilon\|^2 + \int_0^1 \mu|g_0(\mu)|^2 \mathrm{d}\mu + \int_{-1}^0 |\mu|g_Z(\mu)|^2 \mathrm{d}\mu) \tag{35}$$

and the solution of the general problem with $\epsilon > 0$ non zero, f and non zero (g_0 and g_Z), follows by linearity. The above construction will be used to prove convergence of the numerical method in the second part of the paper.

Existence of a solution for $\epsilon = 0$

To let $\epsilon \to 0$, one proceeds with the following contradiction argument. If there would be no finite constant C for which holds the relation:

$$\|\tilde{I}_\epsilon\|^2_{L^2(\Omega)} \leq C\|f\|^2_{L^2(\Omega)} \tag{36}$$

that would imply the existence of a family of functions f_ϵ of $L^2(\Omega)$ with norm equal to 1 while the corresponding solution of I_ϵ would go to infinity in the same norm. Then it generates a solution to the problem:

$$\tilde{f}_\epsilon = \frac{f_\epsilon}{\|I_\epsilon\|} \to 0 \quad \tilde{I}_\epsilon = \|\frac{I_\epsilon}{\|I_\epsilon\|}\| = 1, \qquad \mu\partial_t \frac{I_\epsilon}{\|I_\epsilon\|} + (\frac{I_\epsilon}{\|I_\epsilon\|} - \frac{1}{2}\int_{-1}^{1}\frac{I_\epsilon}{\|I_\epsilon\|}d\mu) = \frac{f_\epsilon}{\|I_\epsilon\|} \to 0. \tag{37}$$

Now $\tilde{I}_\epsilon$ converge *weakly* to a limit solution of the Milne problem with zero data, hence to 0 by the uniqueness of the solution; To complete (by contradiction) the proof one has to show the *strong* convergence of $\tilde{I}_\epsilon$ which is of norm 1. This follows from the so called *averaging lemma* (cf [15] and [11]) using the estimate.

$$\|\mu\partial_t\tilde{I}_\epsilon\| \leq \|(\frac{I_\epsilon}{\|I_\epsilon\|} - \frac{1}{2}\int_{-1}^{1}\frac{I_\epsilon}{\|I_\epsilon\|}d\mu)\| + O(\epsilon) \tag{38}$$

Proof of the non negativity

Positivity can be shown by the following standard intuitive arguments.

Denote by (τ_+,μ_+) (resp. (τ_-,μ_-) the point where I_ϵ achieves its maximum (resp minimum). Then whenever the maximum (resp. minimum) is reached inside the open set $(0,Z)\times(-1,1)$ one has:

$$\mu\partial_\tau I_\epsilon = 0\,, (I_\epsilon(\tau_+,\mu_+) - \frac{1}{2}\int_{-1}^{1} I_\epsilon(\tau_+\mu)d\mu)) \geq 0 \quad \text{resp.} \quad (I_\epsilon(\tau_-,\mu_- - \frac{1}{2}\int_{-1}^{1} I_\epsilon(\tau_-\mu)d\mu) < 0 \tag{39}$$

And if it is reached on the boundary Σ_+ (resp. Σ_-)one has:

$$(\mu\partial_\tau I)(\tau_+,\mu_+) \geq 0 \quad \text{resp.} \quad (\mu\partial_\tau I)(\tau_-,\mu_-) \leq 0\,. \tag{40}$$

Consequently, the equation:

$$\epsilon I_\epsilon + \mu \partial_\tau I_\epsilon + I_\epsilon - \frac{1}{2}\int_{-1}^{1} I(\tau,\mu)d\mu = f(\tau,\mu) \tag{41}$$

implies that if the data f, g_0 and g_Z are non negative and if the minimum is reached inside the domain it cannot be negative and if reached on Σ_+ by (40) it cannot be negative either. The only remaining case is the situation where this minimum is reached on Σ_- but then it coincides with g_0 or g_Z which both are non negative. Hence in all cases one has

$$I_\epsilon(\tau,\mu) \geq I_\epsilon(\tau_-,\mu_-) \geq 0 \tag{42}$$

In the same way for the solutions of the problem

$$\epsilon I_\epsilon + \mu \partial_\tau I_\epsilon + I_\epsilon - \frac{1}{2}\int_{-1}^{1} I_\epsilon(\tau,\mu)d\mu = 0, \tag{43}$$

$$\text{with} \quad g_0(\mu) \geq 0 \quad \text{and } g_Z(\mu) \geq 0, \tag{44}$$

a positive maximum cannot be reached inside the domain because with (40) it should be negative which contradict (44) , and it cannot be reached on Σ_+ by the same argument since I_ϵ coincides with $g_0(\mu)$ or $g_Z(\mu)$. Since the above properties are independent of ϵ the proof of the positivity and of the estimate (23b) follow by letting $\epsilon \to 0$. □

Remark 3 *For the above problem L^∞ estimates and positivity for I or I_ϵ are even more natural than L^2 estimates. However, to produce a complete mathematical proof one proceeds as follow:*

1. *Observe that the above estimates are fully valid for C^1 solutions.*
2. *Use the fact that smooth solutions with smooth data are dense in the set of solutions and that the above estimates remain valid under weak limit.*

This approach is documented with details and used in [1].

To conclude this section it is convenient to recall the implicit formula for the solution of the problem :

Proposition 3 *Let $J(\tau) = \frac{1}{2}\int_{-1}^{1} I(\tau,\mu)d\mu$. The solution of (22) with (21) satisfies*

$$\begin{aligned} I(\tau,\mu) = {} & \mathbf{1}_{\mu>0}\Big(\frac{1}{\mu}\mathrm{e}^{-\frac{\tau}{\mu}} g_0(\mu) + \int_0^\tau \mathrm{e}^{-\frac{\tau-t}{\mu}}\big(J(t)+f(t,\mu)\big)\frac{dt}{\mu}\Big) \\ & + \mathbf{1}_{\mu<0}\Big(\frac{1}{|\mu|}\mathrm{e}^{-\frac{Z-\tau}{|\mu|}} g_Z(\mu) - \int_\tau^Z \mathrm{e}^{-\frac{Z-\tau}{|\mu|}}\big(J(t)+f(t,\mu)\big)\frac{dt}{|\mu|}\Big). \end{aligned} \tag{45}$$

This formula under different variants will be used below.

4.1 Milne Problem and "non explicit formula" for the temperature in term of the albedo of the Earth

The fraction of the incoming solar energy scattered by Earth back to space is referred to as the planetary albedo and is an essential component of the Earth energy balance; cf. for instance [26]. In particular it can be combined with Milne problem to determine the temperature of the Earth as described below.

Hence in $(0,Z)\times(-1,1)$ one considers an intensity of radiation which evolves according to the equation:

$$\mu \partial_\tau I + I - \frac{1}{2}\int_{-1}^{1} I(\tau,\mu')d\mu' = 0 \tag{46}$$

Then on the upper atmosphere $\tau = Z$ an incoming boundary condition is given, for instance:

$$I(\tau,\mu)|_{\mu<0} = |\mu| I_\infty \tag{47}$$

with I_∞ representing the intensity of the radiation coming from the Sun.

On the surface of the Earth ie for $\tau = 0$ the amount of radiation scattered back in the atmosphere $I(0,\mu)|_{\mu>0}$ depends on the incoming radiation $I(0,\mu)_{\mu<0}$. Therefore one assumes that it is given by the albedo operator $\mathcal{A}$:

$$I(Z,\mu)|_{\mu<0} = \mathcal{A}\big(I(Z,\mu)_{|\mu>0}\big) \tag{48}$$

Such operator may depend on many parameters in a very complex fashion (cf. the discussion in section 2.2 of [26]). However, in the present setting of the Milne problem we assume that $\mathcal{A}$ – which is a data of the problem– is a linear contraction operator in the $|\mu|^{\frac{1}{2}}$ weighted Sobolev spaces:

$$\mathcal{A} : L^2(|\mu|^{\frac{1}{2}}, (-1,0)) \mapsto L^2(\mu^{\frac{1}{2}}, (0,1)), \qquad \|\mathcal{A}(I)\| \leq \|I\| . \tag{49}$$

Then one has the following:

Theorem 2

1. *In $\Omega = (0,Z)\times(-1,1)$ the problem*

$$\mu\partial_\tau I + I - \frac{1}{2}\int_{-1}^{1} I(\tau,\mu')d\mu' = 0 \tag{50}$$

with the incoming data

$$I(Z,\mu)|_{\mu<0} = |\mu| I_\infty \tag{51}$$

and the albedo data

$$I(0,\mu)|_{\mu>0} = \mathcal{A}(I(0,\mu)_{|\mu<0}) \tag{52}$$

has a unique solution $I_{\mathcal{A}} \in L^2((0,Z)\times(-1,1))$.

2. *According to the Stefan Boltzmann law the temperature on the Earth is given by the formula:*

$$T = \Big(\frac{C(Z,\mathcal{A})}{\sigma}\Big)^{\frac{1}{4}} I_\infty^{\frac{1}{4}} \tag{53}$$

with $C(Z,\mathcal{A})$ denoting a constant depending on the depth of the atmosphere Z and the albedo operator $\mathcal{A}$.

Proof : The proof follows the same principles as above: It is based on the formula, obtained by multiplication by I and integration over Ω :

$$\begin{aligned} 0 = \int_\Omega (\mu\partial_\tau I + I - \frac{1}{2}\int_{-1}^{1} I(\tau,\mu')d\mu')I(\tau,\mu)d\mu = \int_0^Z \int_{-1}^{1} \Big(I - \frac{1}{2}\int_{-1}^{1} I(\tau,\mu')d\mu')I(\tau,\mu)\Big)^2 d\mu d\tau \\ + \frac{1}{2}\int_{-1}^{0} |\mu|(I(0,\mu))^2 \mathrm{d}\mu - \frac{1}{2}\int_0^1 \mu(I(0,\mu))^2\mathrm{d}\mu + \frac{1}{2}\int_0^1 \mu(I(Z,\mu))^2\mathrm{d}\mu - \frac{1}{2}\int_{-1}^{0}|\mu|(I(Z,\mu))^2\mathrm{d}\mu \end{aligned} \tag{54}$$

On the other hand one has

$$\frac{1}{2}\int_0^1 \mu(I(Z,\mu))^2\mathrm{d}\mu - \frac{1}{2}\int_{-1}^{0}|\mu|(I(Z,\mu))^2\mathrm{d}\mu \geq -\frac{1}{2}\int_{-1}^{0}|\mu|(I(Z,\mu))^2\mathrm{d}\mu \geq -\frac{1}{4}I_\infty \tag{55}$$

and with the contraction property of the albedo operator:

$$\frac{1}{2}\int_{-1}^{0} |\mu|(I(0,\mu))^2\mathrm{d}\mu - \frac{1}{2}\int_0^1 \mu(I(0,\mu))^2\mathrm{d}\mu \geq \frac{1}{2}\int_{-1}^{0} |\mu|(I(0,\mu))^2\mathrm{d}\mu - \frac{1}{2}\int_0^1 \mu(\mathcal{A}(I(0,\mu)_{|\mu<0}))^2\mathrm{d}\mu \ \geq 0 \tag{56}$$

eventually one obtains the estimate:

$$\int_0^Z \int_{-1}^1 \big(I - \frac{1}{2}\int_{-1}^1 I(\tau,\mu')d\mu' I(\tau,\mu)\big)^2 d\mu d\tau \ \leq \frac{1}{4} I_\infty \,. \tag{57}$$

This gives the uniqueness of the solution. Existence follows by the same ϵ regularization as above concluding the proof of point 1. For point 2 one observes that the mapping $I(Z,\mu)|_{\mu<0} \mapsto I(0,\mu)$ is in the above setting, uniquely well defined and linear and hence one has:

$$\int_{-1}^1 I(0,\mu)\mathrm{d}\mu = C(Z,\mathcal{A})I_\infty \tag{58}$$

where as indicated $C(Z,\mathcal{A})$ depends only on the depth of the atmosphere and of the albedo operator. Then the Stefan-Boltzmann law gives (53). □

Remark 4

- *Observe that the above analysis can be applied with almost no modification to the case where the hypothesis (51) for the incoming radiation is replaced by*

$$I(0,\mu)|_{\mu>0} = \phi(\mu)I_\infty \quad \text{where } \phi \text{ is given in } L^2(\mu^{\frac{1}{2}},(0,1))\,. \tag{59}$$

  However, $C(Z,\mathcal{A})$ is replaced by a coefficient $C(Z,\phi,\mathcal{A})$ which may depend on ϕ in a less explicit and more subtle way.

- *The case where no radiation is reemitted (in other world where all the radiation is absorbed by the Earth) fits simply in the above discussion with $\mathcal{A} = 0$.*

- *The case where the earth acts like a mirror reemitting all the incoming radiation fits also simply in the above discussion with*

$$I(0,\mu)|_{\mu>0} = I(0,-\mu)|_{\mu>0} = \mathcal{A}(I(0,\mu)_{\mu<0}). \tag{60}$$

- *To describe a situation where a certain fraction α (Maxwell accommodation coefficient) of the radiation is reemitted while the rest is homogenized, maintaining the total intensity equal to 0 , one introduces the albedo operator.*

$$I(0,\mu)|_{\mu>0} = \mathcal{A}(I(0,\mu)|_{\mu<0}) = \alpha I(0,-\mu) + (1-\alpha)\int_0^1 I(0,-\mu)d\mu \tag{61}$$

  which satisfies the hypothesis of the theorem 2 and leads to a constant $C(Z,\alpha)$. In particular this accommodation coefficient may depend on the temperature T and that would lead, for the temperature to an even more implicit equation of the form (53) with a temperature dependent operator $\mathcal{A}(T)$ for instance with the accommodation coefficient given as a function of the earth $T \mapsto \alpha(T)$

$$\sigma T^4 = \int_{-1}^0 I(0,\mu)\,d\mu + \int_0^1 \mathcal{A}(\alpha(T), I(0,\mu)_{\mu<0})(\mu)\,d\mu \tag{62}$$

5 The half-space Milne problem

Let us study the case $Z = +\infty$, the so-called half-space Milne problem. For the Milne equation (46), define the flux by $\Phi_I := \int_{-1}^1 \mu I(\tau;\mu')d\mu'$. Then one has

$$\frac{d}{d\tau}\Phi_I(\tau) = 0 \quad \text{and} \quad \frac{d}{d\tau}\int_{-1}^1 \mu^2 I(\tau;\mu')d\mu' + \Phi_I(\tau) = 0 \tag{63}$$

As a consequence to remain uniformly bounded with respect to τ for $Z \to \infty$ any solution of (64) has to have $\Phi_I = 0$. This justifies the following (cf.([6] and [5])

Theorem 3 *For any incoming data $g_0(\mu)$ defined for $\tau = 0$ and $\mu \in (0,1)$ with $g_0(\mu) \in L^2(\mu^{\frac{1}{2}}, (0,1))$, there exists a unique uniformly bounded in τ solution of the half space Milne problem:*

$$\mu \partial_\tau I + I - \frac{1}{2}\int_{-1}^{1} I(\tau,\mu')d\mu' = 0, \quad \forall \tau \in \mathbb{R}^+, \quad I(0,\mu)|_{\mu>0} = g_0(\mu)\,. \tag{64}$$

This solution has zero flux and satisfies the estimates:

$$\sup_{\tau\geq 0, \mu\in(-1,1)} |I(\tau,\mu)| \leq \sup_{\mu\in(0,1)} |g_0(\mu)| \text{ and } \int_0^\infty e^{\alpha\tau}\int_{-1}^{1}(I-\frac{1}{2}\int_{-1}^{1} I)^2 d\mu' \leq \frac{1}{1-\alpha}\int_0^1 \mu|g(0,\mu)|^2|d\mu, \quad \forall \alpha \in [0,1). \tag{65}$$

This solution converges exponentially fast to a constant $C(g_0)$; moreover the mapping $g \mapsto C(g)$ is linear continuous from $L^2(|\mu|^{\frac{1}{2}}, (0,1))$ into $\mathbb{R}$.

Proof : Once again the proof is only sketched below; for details see [5]. First one considers the solution on a double domain $(0,2Z)\times(-1,1)$ with incoming boundary data $I(2Z,\mu)|_{\mu<0} = g_0(-\mu)$. This makes the solution of (46) unique, well defined and symmetric with respect to $Z\times(-1,1)$ in the sense

$$\forall\{|z| < Z, \mu \in (-1,1)\} \quad I(Z-z,\mu) = I(Z+z,-\mu)\,.$$

Hence, $\Phi_I(Z) = \int_{-1}^{1}\mu I(Z,\mu)\mathrm{d}\mu = 0$. Since $\Phi_I(\tau)$ is independent of τ, it is equal to 0 everywhere.

Then the decomposition of I into its average $I_a(\tau) = \frac{1}{2}\int_{-1}^{1} I(\tau,\mu')d\mu'$ and the orthogonal complement $I_{ort} = I - \frac{1}{2}\int_{-1}^{1} I(\tau,\mu')d\mu'$ gives, with the 0-flux property, the relation:

$$\int_{-1}^{1}\mu I^2(\tau,\mu)\mathrm{d}\mu = \int_{-1}^{1}\left(I(\tau,\mu) - \frac{1}{2}\int_{-1}^{1} I(\tau,\mu')d\mu'\right)^2 d\mu \tag{66}$$

Multiplying the equation by $e^{\alpha\tau}I$ with $0<\alpha<1$ and integrating on $(0,Z)\times(0,1)$ with the relation:

$$e^{\alpha\tau}\int_{-1}^{1}(\mu\partial_\tau I)I\mathrm{d}\mu = \partial_\tau(e^{\alpha\tau}\frac{1}{2}\int_{-1}^{1}\mu I^2\mathrm{d}\mu)) - \alpha e^{\alpha\tau}\frac{1}{2}\int_{-1}^{1}\mu I^2\mathrm{d}\mu. \tag{67}$$

Thus, one obtains the estimate:

$$(1-\alpha)\int_0^Z e^{\alpha\tau}\int (I(\tau,\mu) - \frac{1}{2}\int_{-1}^{1} I(\tau,\mu')d\mu')^2 d\mu)d\tau \leq \int_0^1 \mu|g_0(\mu)|^2 d\mu. \tag{68}$$

With (46) one can show that it gives the exponential convergence to a constant $C(g)$ for $Z\to\infty$.

The uniqueness of the solution is based on the same type of estimates. □

Remark 5 *The determination of $g \mapsto C(g)$ and in the quest for an explicit or semi explicit formula has been in the last century the object of intensive activities involving in particular the Wiener-Hopf calculus (cf. [7]). However, the most explicit form is based on the introduction of the Chandrasekhar function H, defined by the implicit formula:*

$$H(\mu) = 1 + \frac{1}{2}\mu H(\mu)\int_0^1 \frac{H(\mu')}{\mu+\mu'}d\mu', \tag{69}$$

which gives the constant $C(g)$ by the relation

$$C(g) = \frac{\sqrt{3}}{2}\int_0^1 \mu' H(\mu')g(\mu')d\mu'\,. \tag{70}$$

In particular for $g(\mu) = \mu$ one has $\overline{\omega_1} := C(\mu) = 0.7014$.

5.1 Approximate determination of the temperature on Earth

We present an approximation which yield a temperature on Earth based on the asymptotic behaviour of the half-space Milne problem.

5.1.1 Using Theorem 3

We return to climate dynamics where $r \in (0, H)$ is the altitude but not in an evanescent atmosphere, i.e. (14) without the Chandrasekhar correction. We make the following change of variable

$$y(r) = \int_0^r \kappa\rho(r')\mathrm{d}r'$$

and assume that $r \mapsto \rho(r)$ does not decrease too fast so that $y(+\infty) = +\infty$. Then we focus on the case $H >> 1$. One observes that $I(y, \mu)$ is solution of the Milne equation (64) for $y \in \mathbb{R}^+$, $\mu \in (-1, 1)$ with . Assume constant flux given by

$$\tilde{\Phi} = \int_{-1}^{1} \mu(y - \mu)d\mu = -\frac{2}{3} \tag{71}$$

Hence one introduces the solution $e(y, \mu)$ of the half space problem with 0 flux and equal to μ at $y = 0$ for $\mu > 0$. As was proved in theorem 3 such solution exists is unique and converges exponentially fast to the constant $\overline{\omega_1}$ as y goes to ∞. As such, for some small function rem,

$$I = c[y - \mu + \mathrm{r}em(y, \mu)] \tag{72}$$

provides a *boundary layer approximation* (ie for $y > 0$, $y << 1$) of the solution of the Milne problem with a flux given equal to $\frac{2}{3}c$ and no incoming radiation for $y = 0$ and r$em(y, \mu)$ going exponentially fast to $\overline{\omega_1}$ when $y \to \infty$. Hence for y large enough one has

$$I(y, \mu)|_{\mu<0} = c[y - \mu + \overline{\omega_1}] + o(\mathrm{e}^{-\alpha y}) \tag{73}$$

Now let us use the linearity of the solution with respect to the data and consider the same problem with incoming intensity without the term $o(\mathrm{e}^{-\alpha Z})$. As this is a small perturbation we expect to solution at $y = 0$ to be

$$I(0, \mu) \approx c[-\mu + \overline{\omega_1}]. \tag{74}$$

Consequently,

$$\int_{-1}^{1} I(0, \mu))\mathrm{d}\mu \simeq c \int_{-1}^{0} ((-\mu) + \overline{\omega_1})d\mu = \frac{c}{2} + c\overline{\omega_1} \tag{75}$$

For a solar flux equal to Φ the intensity I_{Earth} is obtained after multiplication by $\frac{3}{2}\Phi$ (see (71). This gives:

$$\int_{-1}^{1} I_{Earth}(\mu)d\mu \simeq \frac{3}{4}\Phi(1 + 2\overline{\omega_1}) \tag{76}$$

and with the Stefan-Boltzmann law one obtains:

$$T_{Earth} \simeq \left(\frac{3}{8\sigma}\Phi(1 + 2\overline{\omega_1})\right)^{\frac{1}{4}} \tag{77}$$

Formula (77) with $\Phi = Q(1 - a)/4$ as in [13] eq (2.2) p66, gives $T = 351K$.

6 Numerical analysis

Consider (16), adimentionalised and without the Chandrasekhar correction::

$$\mu\frac{\partial I_\nu}{\partial\tau}+\kappa_\nu\left(I_\nu-B_\nu(T(\tau))\right)=0,\ \ \forall\{\tau,\mu\}\in(0,Z)\times(-1,1),\forall\nu\in\mathbb{R}^+, \tag{78}$$

$$B_\nu(T)=\frac{\nu^3}{\mathrm{e}^{\frac{\nu}{T}}-1},\qquad \int_0^\infty\kappa_\nu\left(B_\nu(T(\tau))-\frac{1}{2}\int_{-1}^1 I_\nu\mathrm{d}\mu\right)d\nu=0,\ \ \forall\tau\in(0,Z), \tag{79}$$

$$I_\nu(Z,\mu)|_{\mu<0}=0,\qquad I_\nu(0,\mu)|_{\mu>0}=\mu Q_0 B_\nu(T_{Sun}). \tag{80}$$

The physical constants are given in Table 1. Following (14)(15), we set $\nu_0=10^{14}$ so that for the computations $\nu\in(0.01,20)$ is enough; we choose $B_0=\frac{2\hbar\nu_0^3}{c^2}=1.47\,10^{-8}$ and $T_0=\frac{\hbar\nu_0}{k}=4798$; then the physical quantities (noted with a breve) are recovered by $\breve{T}=T_0T$, $\breve{B}_\nu(T)=B_0B_\nu(T)$, $\breve{I}_\nu=B_0I_\nu$. Similarly we choose $\lambda=10^3$ and set $\kappa_\nu=\lambda\rho_0\breve{\kappa}_\nu=1.225\breve{\kappa}_\nu$. Thus, in the computations, $H=12$ and $R=40000$; but R does not appear if the Chandraskhar correction is neglected.

The energy of sunlight is $1370\mathrm{Wm}^{-2}$, so, in Paris, $\cos\theta=1/\sqrt{2}$, with $a=0.36$, $Q=1370(1-a)/\sqrt{2}=620$. Furthermore $T_{Sun}=5.4/4.798=1.126$.

If κ_ν is independent of ν then $\bar{I}=\int_0^\infty I_\nu\mathrm{d}\nu$ may be computed by (20) with $g_Z=0$ and T be given by

$$T(\tau)=\left(\frac{Q}{2\sigma_b}\int_{-1}^1 I(\tau,\mu)\mathrm{d}\mu\right)^{\frac{1}{4}},\quad \sigma_b=\frac{B_0\nu_0}{15}\left(\frac{\pi}{T_0}\right)^4 \tag{81}$$

Table 1: *The physical constants.*

c	$\hbar$	k	ρ_0	R	H	σ_b
$2.998\,10^8$	$6.6261\,10^{-34}$	$1.381\,10^{-23}$	$1.225\,10^{-3}$	$4\,10^7$	$12\,10^3$	$1.801\,10^{-8}$

6.1 Compatiblity with the Milne equation

Without dimensional scaling, with $\kappa_\nu=\kappa$ constant, the total intensity is given by

$$\mu\partial_\tau\bar{I}+\kappa(\bar{I}-\frac{1}{2}\int_{-1}^1\bar{I})=0,\quad \bar{I}(0,\mu)|_{\mu>0}=\mu Q,\quad \bar{I}(Z,\mu)|_{\mu<0}=0 \tag{82}$$

This comes from an integration in ν of

$$\mu\partial_\tau\breve{I}_\nu+\kappa_\nu(\breve{I}_\nu-\breve{B}_\nu)=0,\quad \int_0^\infty\kappa_\nu(\breve{B}_\nu-\frac{1}{2}\int_{-1}^1\breve{I}_\nu)=0,\quad \breve{I}(0,\mu)|_{\mu>0}=\mu Q_0\breve{B}_\nu(\breve{T}_{Sun}),$$

with $\breve{I}(Z,\mu)|_{\mu<0}=0$. Indeed, an integration with respect to ν yields

$$\mu\partial_\tau\bar{I}+\kappa(\bar{I}-\bar{B})=0,\quad \kappa(\bar{B}-\frac{1}{2}\int_{-1}^1\bar{I})=0,\quad \bar{I}(0,\mu)|_{\mu>0}=\mu Q_0\int_0^\infty\breve{B}_\nu(\breve{T}_{Sun})\mathrm{d}\nu.$$

Hence we must have

$$Q_0\int_0^\infty\breve{B}_\nu(\breve{T}_{Sun})\mathrm{d}\nu=Q_0\sigma_b\breve{T}_{Sun}^4=Q,\quad\Rightarrow Q_0=\frac{Q}{\sigma_b\breve{T}_{Sun}^4}=4.036\,10^{-5}.$$

Adimensionalisation sets $I_\nu=\breve{I}_\nu/B_0$, so the system becomes (83):

6.1.1 The adminensionalised problem

$$\mu\partial_\tau I_\nu + \kappa_\nu(I_\nu - B_\nu(T)) = 0, \quad \int_0^\infty \kappa_\nu(B_\nu(T) - \frac{1}{2}\int_{-1}^{1} I_\nu) = 0, \quad B_\nu(T) = \frac{\nu^3}{e^{\frac{\nu}{T}} - 1}, \text{ in } (0,Z)\times(-1,1) \tag{83}$$

with $I_\nu(Z,\mu)|_{\mu<0} = 0$, $I(0,\mu)|_{\mu>0} = \mu Q_\nu := Q_0\mu B_\nu(T_{Sun})$, $Z = 1 - e^{-12}$ and $T_{Sun} = 1.126$, $Q_0 = 4.036\,10^{-5}$.

6.2 Numerical scheme

For (83), two numerical schemes are used. Both need the following fixed point iterations:

$$\mu\partial_\tau I^{n+1} + \kappa(I^{n+1} - B^n) = 0, \quad B^{n+1}(\tau) = \frac{1}{2}\int_{-1}^{1} I^{n+1}. \tag{84}$$

The first one, refered below as "implicit", is based on a discretization of the exact solution of the equation from I^{n+1}:

$$I^{n+1} = \mathbf{1}_{\mu>0}\left[\mu e^{-\kappa\nu\frac{\tau}{\mu}} + \int_0^\tau \frac{e^{\kappa\frac{t-\tau}{\mu}}}{\mu}\kappa B^n dt\right] + \mathbf{1}_{\mu<0}\int_\tau^Z \frac{e^{\kappa\frac{t-\tau}{\mu}}}{\mu}\kappa B^n(t)dt, \quad B^{n+1}(\tau) = \frac{1}{2}\int_{-1}^{1} I^{n+1}d\mu. \tag{85}$$

Programming is straightforward; it needs only to be evaluated at all vertices of a triangulation of the rectangle Ω. The integrals are approximated by a second order quadrature (trapezoidal rule) on a non uniform discretization of $(0,Z)$ to account for the tiny interval where infrared radiations occur. Table 2 shows the error versus the mesh size for example 6.2.1, below. Note however that the precision is weak: $O(h)$, probably because the solution is singular at $\mu = 0$.

The second method is based on a finite element discretization of the PDE as in [17]. It uses a weak formulation of (83) discretized in V_h, the space of Lagrangian-P^1 triangular elements. For stability a least square upwinding term (SUPG) is added, namely $h_{\text{SUPG}}(\mu\partial_\tau I + \kappa I)(\mu\partial_\tau\hat{I} + \kappa\hat{I})$ for a small h_{SUPG}, where $\hat{I}$ is the test function of the variational formulation. This means that at each iteration n of a fixed point loop one must solve

$$\int_\Omega \left(\kappa I^{n+1}\hat{I} + \mu\partial_\tau I^{n+1} + h_{\text{SUPG}}(\mu\partial_\tau I^{n+1} + \kappa I)(\mu\partial_\tau\hat{I}^{n+1} + \kappa\hat{I})\right) = \int_\Omega \kappa B^n\hat{I}, \tag{86}$$

with $I^{n+1} \in V_h$ satisfying the boundary conditions and for all $\hat{I} \in V_h$ with $\hat{I}(0)|_{\mu>0} = I(Z)|_{\mu<0} = 0$. The method has been implemented using `FreeFem++`[18], which uses the library `UMFPACK` [12] to solve the linear systems. We found that the method works best when the triangulation is build first in the physical variables r,ϕ and then mapped to the rectangle of τ,μ. The automatic mesh refinement of `FreeFem++`, which is based on the Hessian of I^n here, is also convenient to improve precision.

6.2.1 Example and performance:

$B_\nu(t) = t$, $\kappa_\nu = 1$, $Q_\nu = 1 \Rightarrow I_\nu = \mathbf{1}_{\mu>0}\left[2\mu e^{-\frac{\tau}{\mu}} - \mu\right] - \mathbf{1}_{\mu<0}\left[\mu(1 - e^{\frac{(Z-\tau)}{\mu}})\right]$. The performance of both methods are reported in Table 2. The Finite element method (86) appears to be less precise than (85), but much faster. Adjustment of h_{SUPB} is done once and for all proportionally to the number of points on $\partial\Omega$.

Table 2: Numerical error versus mesh size h on Example 1: the error is $O(h)$

Number of Vertices	1107	4008	9856
L^2-error by FEM	$20.\,10^{-4}$	$7.7\,10^{-4}$	$3.7\,10^{-4}$
L^2-error by (85)	$14.\,10^{-4}$	$0.45\,10^{-4}$	$0.12\,10^{-4}$

6.2.2 Convergence of the iterative scheme

For clarity let $\kappa = 1$. Scheme (84) is modified slightly with a parameter ϵ

$$\mu\partial_\tau I^{n+1} + (1+\varepsilon)I^{n+1} = \frac{1}{2}\int_{-1}^{1} I^n \mathrm{d}\mu$$

As observed in [1] and [2] solutions of scalar kinetic equation with 0 incoming data are 0 viscosity limit of elliptic equations; therefore it is natural to introduce such regularization in (86).

Adding the terms with ϵ makes also the convergence proof rather simple. Indeed, as for the derivation of (34)

$$\mu\partial_\tau(I^{n+1} - I^n) + (1+\varepsilon)(I^{n+1} - I^n) = \frac{1}{2}\int_{-1}^{1}(I^n - I^{n-1})\mathrm{d}\mu$$

Consequently,

$$\begin{aligned}
& \int_\Omega \frac{\mu}{2}\partial_\tau(I^{n+1} - I^n)^2 + (1+\varepsilon)\int_\Omega (I^{n+1} - I^n)^2 = \int_\Omega (I^{n+1} - I^n)(I^n - I^{n-1}) \\
\Rightarrow \quad & \int_{-1}^{1} \mu|I^{n+1} - I^n|^2 \mathrm{d}\mu\Big|_0^Z + (1+\varepsilon)\|I^{n+1} - I^n\|_{0,\Omega}^2 \le \|I^{n+1} - I^n\|_{0,\Omega}\|I^n - I^{n-1}\|_{0,\Omega} \\
\Rightarrow \quad & \|I^{n+1} - I^n\|_{0,\Omega} \le \frac{1}{(1+\varepsilon)}\|I^n - I^{n-1}\|_{0,\Omega} \le \frac{1}{(1+\varepsilon)^n}\|I^1 - I^0\|_{0,\Omega}
\end{aligned}$$

6.2.3 Results

In practice the convergence is much faster than predicted above, even with $\epsilon = 0$, as shown by Table 3. A typical result is also shown, in the physical coordinates, on figure 4 for (82) with $Q = 1$. It shows the solution of the Milne problem computed on a grid 40×20. The temperature on Earth, given by (81), is $T = 298K$.

Table 3: Convergence of the fixed point algorithm with $\kappa_\nu = 1$.

Iteration	1	2	3	4	5
$\|I^{n+1} - I^n\|_0^2$	0.524721	0.0315412	0.00777077	0.00188975	0.000457752

6.3 The Chandrasekhar equation

For a grey atmosphere the model with the Chandrasekhar correction reduces to

$$\mu\partial_\tau I + \kappa I + \gamma\partial_\mu I = \frac{\kappa}{2}\int_{-1}^{1} I\mathrm{d}\mu, \quad \forall \tau, \mu \in \Omega := (0, Z)\times(-1, 1) \tag{87}$$

and (11). The two schemes above are easily modified to accommodate γ. For the FEM scheme one just adds to (86) $\gamma(\tau,\mu)\hat{I}\partial_y I$ under the left integral of (86) plus an upwinding term like (89) below.

The implicit scheme is modified as follows:

$$\begin{aligned}
&.(1) \quad B^n(\tau) = \frac{1}{2}\int_{-1}^{1} I^n(\tau,\mu)\mathrm{d}\mu, \\
&.(2) \quad I^{n+\frac{1}{2}} = \mathbf{1}_{\mu>0}\left[\mu \mathrm{e}^{-\kappa\frac{\tau}{\mu}} + \int_0^\tau \frac{\mathrm{e}^{\kappa\frac{t-\tau}{\mu}}}{\mu}\kappa B_\nu^n(t)\mathrm{d}t\right] - \mathbf{1}_{\mu<0}\int_\tau^Z \frac{\mathrm{e}^{\kappa\frac{t-\tau}{\mu}}}{\mu}\kappa B_\nu^n(t)\mathrm{d}t, \\
&.(3) \quad \int_\Omega (I^{n+1} + \gamma\partial_\mu I^{n+1})\hat{I} = \int_\Omega I^{n+\frac{1}{2}}\hat{I}, \quad \forall \hat{I} \in V_h, \text{ with boundary conditions (11).}
\end{aligned} \tag{88}$$

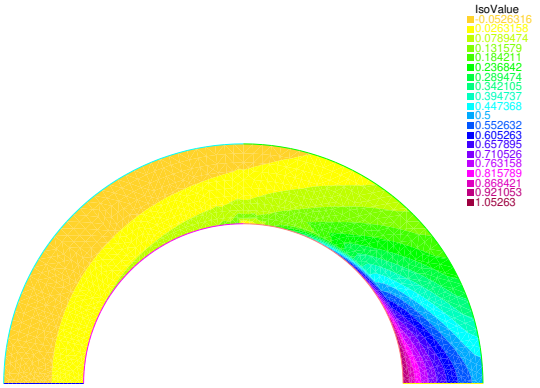

Figure 4: Light intensity level map in the physical domain, i.e. for all ϕ and r. Even though the cercle has radius $R = 3H$, this is not a plot on a cross section of the planet. It shows $I(r, \phi)$ for $r \in (0, H)$ and $\phi \in (-\pi, \pi)$.

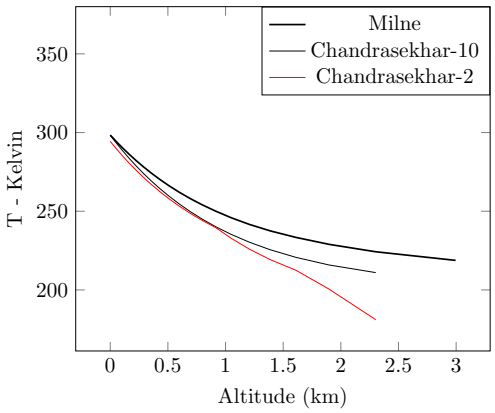

Figure 5: Temperature computed with the Milne and Chandrasekhar equations. In the later case the Earth radius is 2 or 10 times the atmosphere thickness.

This scheme is consistent because $I^{n+\frac{1}{2}}$ satisfies $\frac{\mu}{\kappa}\partial_\tau I^{n+\frac{1}{2}} + I^{n+\frac{1}{2}} = B^n$ and adding this to the last equation above gives $I^{n+1} + \frac{\gamma}{\kappa}\partial_\mu I^{n+1} + \frac{\mu}{\kappa}\partial_\tau I^{n+\frac{1}{2}} = B^n$.

In practice some additional artificial viscosity of amplitude δ should be added on the left in (88)

$$\int_\Omega \frac{\delta}{2}\left(|\mu|\partial_\tau I \partial_\tau \hat{I} + |\gamma|\partial_\mu I \partial_\mu \hat{I}\right) \tag{89}$$

When the above is discretized by a P^1 Finite Element Method, the convergence of the fixed point algorithm is equally fast; results are shown on figure 5 and illustrate the convergence of the solution of Chandrasekhar equations to the solution of the Milne equation when R increases.

7 Numerical simulation of the greenhouse effect

Our aim is to compare the Earth surface temperature for two different functions $\nu \to \kappa_\nu^i(\nu)$, $i = 1, 2$ and observe the relative change of temperature.

The problem is defined in (83); the Chandrasekhar correction is not needed because $R >> H$. To complete the definition of the problem, the values of κ_ν are as follows.

The atmosphere is fairly, but not fully, opaque except in a region $(\nu_1, \nu_2) = (0.2, 0.3)$ where it is much less opaque. If a change in GHG proportion makes the atmosphere more opaque in this range then we may set

$$\kappa_\nu^1 = \kappa_0 - \delta\kappa\, \mathbf{1}_{\nu\in(\nu_1,\nu_2)}, \quad \kappa_\nu^2 = \kappa_0, \quad \Rightarrow \quad \delta\kappa_\nu := \kappa_\nu^2 - \kappa_\nu^1 = \delta\kappa\, \mathbf{1}_{\nu\in(\nu_1,\nu_2)} \tag{90}$$

We chose $\kappa_0 = 1.225$ because of the numerical value of the density of air (see (15). We choose arbitrarily $\delta\kappa = 0.5$. The values for ν_1 and ν_2 are on the left side of the Boltzmann curve for Earth, shown in figure 6. In one computation the infrared clear window is narrow: $(\nu_1, \nu_2) = (0.2, 0.3)$. In another it is wider $(\nu_1, \nu_2) = (0.1, 0.4)$.

The computer programs produce 4 temperatures $\tau \mapsto T^j(\tau), j = 0, \ldots, 3$.

1. T^0 is the solution of the Milne equation with $\kappa = \kappa_0 = 1.225$.
2. T^1 is the solution of the multi-group problem with $\kappa_\nu = \kappa^1 = 1.225 - 0.5\,\mathbf{1}_{\nu\in(0.2,0.3)}$.
3. T^2 is the solution of the multi-group problem with $\kappa_\nu = \kappa^2 = 1.225$, ideally equal to T^0.

4. T^3 is the solution of the multi-group problem with $\kappa_0 - \delta\kappa\,\mathbf{1}_{\nu\in(0.1,0.4)}$.

According to figure 1 and figure 2, Green House gases increase κ and makes the window which is transparent to infrared radiations narrower. This will be measured by $T^2 - T^1$ and $T^1 - T^3$. The problem needs to be

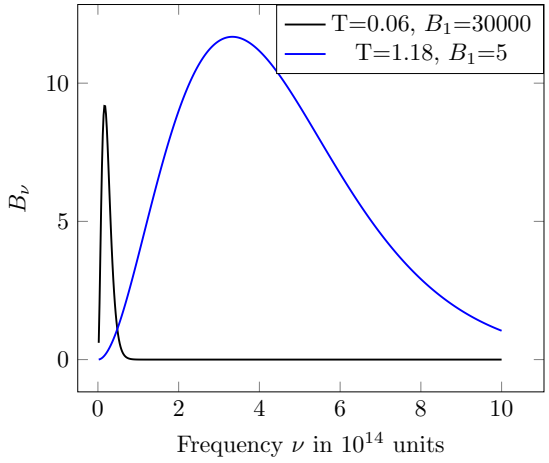

Figure 6: Plot of $B_\nu(T) = \frac{B\nu^3}{e^{\frac{\nu}{T}}-1}$ representing the Light intensities versus ν. The Boltzmann functions plotted, $30000B_\nu(0.06)$ and $5B_\nu(1.18)$ corresponds, to (scaled) emissions from Earth and Sun. The infrared range $\nu \in (0.1, 0.4)$ may be affected by the GHG.

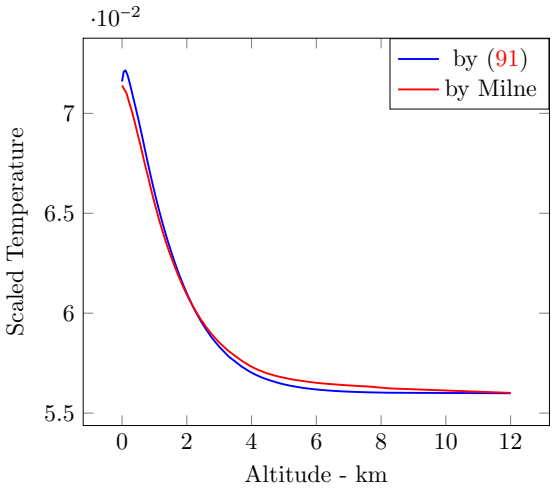

Figure 7: Temperature profile of T^2 computed by solving the multi-group problem (83) compared with the solution of the Milne problem (82 T^0.

discretized in ν by choosing a grid in (ν_m, ν_M), which means that we need to solve the multi-group problem introduced above with (16).

The following numerical scheme is used:

. Set ${K_I}^0 = 0$, choose (ν_m, ν_M) to approximate $(0, \infty)$
for ($n = 0, 1...$){
. Compute $\tau \mapsto T^n(\tau)$ by solving $\int_{\nu_m}^{\nu_M} \kappa_\nu B_\nu(T^n)\mathrm{d}\nu = \frac{1}{2}\int_{-1}^{1} K_I^n \mathrm{d}\mu$; then set $K_I^{n+1} = 0$.
. **for**($\nu = \nu_m; \nu < \nu_M; \nu+ = \delta\nu$){
. Set $B_\nu^n(\tau) = \frac{\nu^3}{e^{\frac{\nu}{T^n(\tau)}}-1}$,
. Solve $\mu\partial_\tau I^{n+1} + \kappa_\nu I^{n+1} = \kappa_\nu B_\nu^n(\tau), \quad I^{n+1}(0,\mu)|_{\mu>0} = \mu Q_0 B_\nu(T_{Sun}), \quad I^{n+1}(H,\mu)|_{\mu<0} = 0.$
. Update ${K_I}^{n+1}+ = \kappa_\nu I_\nu^{n+1}\delta\nu$.
}
} (91)

Finding T^n by inverting the Planck function can be challenging. However, when $\kappa_\nu = \kappa - \delta\kappa\,\mathbf{1}_{(\nu_1,\nu_2)}$ finding T^n, solution of the first equation in (91) can be done by a fixed point k-loop as follows:

$$\int_0^\infty \kappa B_\nu(T^n) - \int_{\nu_1}^{\nu_2} \delta\kappa B_\nu(T^n) = \int_0^\infty \frac{\kappa_\nu}{2}\int_{-1}^{1} I_\nu^n \mathrm{d}\mu\mathrm{d}\nu \;\Rightarrow\; \frac{\kappa\pi^4 {T_{k+1}^n}^4}{15} = \frac{1}{2}\int_{-1}^{1} K_I^n \mathrm{d}\mu + \delta\kappa\int_{\nu_1}^{\nu_2} B_\nu(T_k^n). \quad (92)$$

To assert the method we ask algorithm (91) to recover the solution of the Milne problem (κ_ν constant). The results are shown on figure 7: a precision of 1% is obtained, but refining the mesh and the integration intervals did not improve the precision. This riddle will be solved in section 7.2

Then we computed the relative change of temperature when κ_ν is changed from κ^1_ν to κ^2_ν. The change is of the order of 10^{-2} and negative (see figure 9). In view of the small magnitude of the change, for a verification we turned to a calculus of variations.

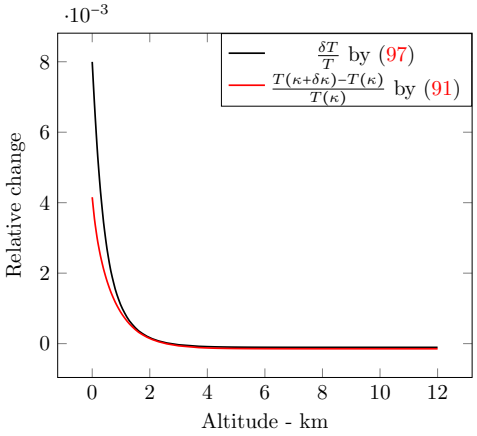

Figure 8: Relative temperature change versus altitude, computed with $\kappa_\nu = 1. + 0.5\,\mathbf{1}_{\nu\in(1,1.5)}$ A direct computation (in red) of the relative change is compared with the result using the calculus of variations (in black). This computation shows that increased opacity in the sunlight range increases the temperature on Earth.

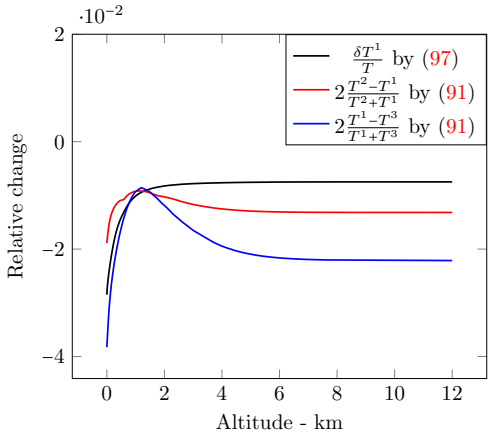

Figure 9: In red and black: relative temperature changes $T^2 - T^1$ versus altitude, when $\kappa^1_\nu = 1.225 - 0.5\,\mathbf{1}_{\nu\in(0.2,0.3)}$ is changed to $\kappa^2_\nu = 1.225$, to account for the GHG opacity. The results using the calculus of variations (see (97)) is compared to a direct simulation of T^1 and T^2. In blue: same but T^3 is computed with κ^1_ν changed to $\kappa^3_\nu = 1.225 - 0.5\,\mathbf{1}_{\nu\in(0.1,0.4)}$ to account for a narrower frequency range of infrared absorption.

7.1 Solution by calculus of variations

Even though both the FEM-based code and the implicit one give the same results, evidently we are trying to observe a temperature variation which is at the limit of the precision of the computer codes (see remark 6 below). So let us try another method.

Let (90) be written as $\kappa_\nu = \kappa + \delta\kappa_\nu$ with $\delta k_\nu = -\delta k\,\mathbf{1}_{\nu\in(\nu_1,\nu_2)}$ and let κ be constant. With the obvious notations of a calculus of variations:

$$\mu\partial_\tau\delta I_\nu + \kappa\delta I_\nu = \kappa\delta B_\nu + \delta\kappa_\nu(B_\nu - I_\nu),\quad \delta I_\nu(0,\mu)|_{\mu>0} = \delta I_\nu(Z,\mu)|_{\mu<0} = 0,$$
$$\int_0^\infty(\delta B_\nu - \frac{1}{2}\int_{-1}^1\delta I_\nu\mathrm{d}\mu)\kappa\mathrm{d}\nu = -\int_0^\infty(B_\nu - \frac{1}{2}\int_{-1}^1 I_\nu\mathrm{d}\mu)\delta\kappa_\nu\mathrm{d}\nu. \tag{93}$$

Let $\delta\bar I = \int_0^\infty \delta I_\nu\mathrm{d}\nu$ and similarly for $\delta\bar B$. Integrating the equations with respect to ν leads to

$$\mu\partial_\tau\delta\bar I + \kappa\delta\bar I - \kappa\delta\bar B = \int_{\nu_1}^{\nu_2}\delta\kappa_\nu(B_\nu - I_\nu)\mathrm{d}\nu,\quad \delta\bar I(0,\mu)|_{\mu>0} = \delta\bar I(Z,\mu)|_{\mu<0} = 0, \tag{94}$$
$$\kappa\left(\delta\bar B - \frac{1}{2}\int_{-1}^1\delta\bar I\mathrm{d}\mu\right) = -\int_{\nu_1}^{\nu_2}\left(B_\nu - \frac{1}{2}\int_{-1}^1 I_\nu\mathrm{d}\mu\right)\delta\kappa_\nu\mathrm{d}\nu. \tag{95}$$

Adding both gives

$$\mu\partial_\tau\delta\bar I + \kappa\delta\bar I - \frac{\kappa}{2}\int_{-1}^1\delta\bar I\mathrm{d}\mu = -\int_{\nu_1}^{\nu_2}\left(I_\nu - \frac{1}{2}\int_{-1}^1 I_\nu\mathrm{d}\mu\right)\delta\kappa_\nu\mathrm{d}\nu. \tag{96}$$

and, knowing that $\delta B = \delta(\frac{\pi^4 T^4}{15}) = 4\frac{\pi^4 T^3}{15}\delta T$, the change in temperature is computed by (95) divided by κ:

$$\frac{4\pi^4 T^3}{15}\delta T = \frac{1}{2}\int_{-1}^{1}\delta\bar{I}\mathrm{d}\mu + \frac{\delta\kappa}{\kappa}\int_{\nu_1}^{\nu_2}\left(B_\nu - \frac{1}{2}\int_{-1}^{1} I_\nu \mathrm{d}\mu\right)\mathrm{d}\nu. \tag{97}$$

The numerical solution of (96) can be obtained both with FEM and the implicit method; results agree roughly and are shown on figure 9. Here too we obtain a decrease of Earth temperature when κ_ν increases in the infrared interval (ν_1, ν_2) and the numerical values of the change obtained are of the same magnitude as those obtained by a direct simulation with κ_ν^1 and κ_ν^2, as seen on figure 9.

7.2 A Formulation to compute only the temperature

These disturbing conclusions forced us to think again and track the precision losses. In doing so we turned to exponential integrals (see `en.wikipedia.org/wiki/Exponential_integral`) to evaluate (88), an idea on which is based the computation of an analytic solution of the Milner problem by complex integrals [13]-Appendix B. Function E_1 is part of the Gnu Scientific Library gsl. One has:

$$\begin{aligned}
&\int_0^1 \mu \mathrm{e}^{-\frac{\kappa\tau}{\mu}}\mathrm{d}\mu = \int_1^\infty x^{-3}\mathrm{e}^{-\kappa\tau x}\mathrm{d}x = E_3(\kappa\tau) = \frac{\mathrm{e}^{-\kappa\tau}}{2}(1-\kappa\tau) + \frac{(\kappa\tau)^2}{2}E_1(\kappa\tau).\\
&\int_0^1 \frac{1}{\mu}\mathrm{e}^{-\frac{\kappa(\tau-t)}{\mu}}\mathrm{d}\mu = \int_1^\infty y^{-1}\mathrm{e}^{-\kappa(\tau-t)y}\mathrm{d}y = E_1(\kappa(\tau-t)),\ t<\tau,\\
&\int_{-1}^0 \frac{1}{\mu}\mathrm{e}^{\frac{\kappa(t-\tau)}{\mu}}\mathrm{d}\mu = -\int_0^1 \frac{1}{\mu'}\mathrm{e}^{\frac{-\kappa(t-\tau)}{\mu'}}\mathrm{d}\mu' = -E_1(\kappa(t-\tau)),\ t>\tau.
\end{aligned} \tag{98}$$

Hence

$$\begin{aligned}
\int_{-1}^1 I_\nu \mathrm{d}\mu \quad &= Q_\nu E_3(\kappa_\nu\tau) + \kappa_\nu\int_0^\tau E_1(\kappa_\nu(\tau-t))B_\nu(t)\mathrm{d}t - \kappa_\nu\int_\tau^Z -E_1(\kappa_\nu(t-\tau))B_\nu(t)\mathrm{d}t\\
&= Q_\nu E_3(\kappa_\nu\tau) + \kappa_\nu\int_0^Z E_1(\kappa_\nu|\tau-t|)B_\nu(t)\mathrm{d}t
\end{aligned} \tag{99}$$

We can modify the iterative scheme (88) because only the flux $F = \int_0^\infty \kappa_\nu \int_{-1}^1 I_\nu \mathrm{d}\mu\mathrm{d}\nu$ is needed. We note also that to compute $\tau \mapsto T^n(\tau)$ when $\kappa_\nu = \kappa_0 - \delta\kappa\,\mathbf{1}_{(\nu_1,\nu_2)}$ by solving

$$\int_{\nu_m}^{\nu_M}\kappa_\nu B_\nu(T^n)\mathrm{d}\nu = \frac{1}{2}F(\tau),$$

amounts to solve, as before iteratively,

$$\kappa_0\frac{\pi^4 T^4}{15} - \delta\kappa\int_{\nu_1}^{\nu_2} B_\nu(T) = \frac{1}{2}F(\tau). \tag{100}$$

Hence, the following iterative scheme:

. Set $F_\nu{}^0 = \int_{\nu_m}^{\nu_M}\kappa_\nu Q_\nu E_3(\kappa_\nu\tau)\mathrm{d}\nu$, where (ν_m, ν_M) approximate $(0,\infty)$
for ($n = 0, 1..$){
. Compute $\tau \mapsto T^n(\tau)$ by solving (100) with F^n
. Then initialize $F^{n+1} = 0$ and
. **for**($\nu = \nu_m; \nu < \nu_M; \nu+ = \delta\nu$){
. $B_\nu^n(t) = \dfrac{\nu^3}{\mathrm{e}^{\frac{\nu}{T^n(t)}} - 1}$, $F^{n+1}+ = \left[Q_\nu E_3(\kappa_\nu\tau) + \kappa_\nu\int_0^Z E_1(\kappa_\nu|\tau-t|)B_\nu^n(t)\mathrm{d}t\right]\kappa_\nu\delta\nu$
}
} \tag{101}

This turns out to be a very fast and easily programmable method and so far the least prone to precision difficulties because the only singular integrand is $E_1(|t|)|_{t\sim 0} \sim -\log(|t|)$; but as it appears under an integral, a dedicated quadrature rule can be used. Discrete Fourier Transform could be used to solve the integral equations but the fixed point iteration process is so fast that it is not worth it.

7.2.1 A new set of tests

In view of the counterintuitive results above an added set of frequencies where tested:

$$\nu \in (1., 1.2) \quad \text{and} \quad \nu \in (1., 1.4). \tag{102}$$

These numbers correspond to absorption rays of the GHG in the lower frequency range of sunlight (see figure 1 and figure 6).

All numerical tests where re-run using(101) (automatic differentiation included) and the same results were obtained (figure 10 & 11): temperature decreases with an narrowed infrared absorption interval, and temperature decreases also when κ_ν is increased in an infrared interval!

However with the new set (102), the temperature increases when κ increases and/or when the partially transparent window decreases in size, yet the numbers are an order of magnitude smaller, about 0.17% at the ground level, i.e. 0.5C.

We note also (figure 10) that we can obtain agreement to at least 3 digits between a direct solution of the Milne problem with constant κ and the same solved by the multi-group problem even though κ is not a function of ν.

Figure 9 and figure 11 are similar, but notice the calculus of variations and the direct simulations of temperature differences could differ by a factor of 2; another indication that we are at the precision limit of these programs.

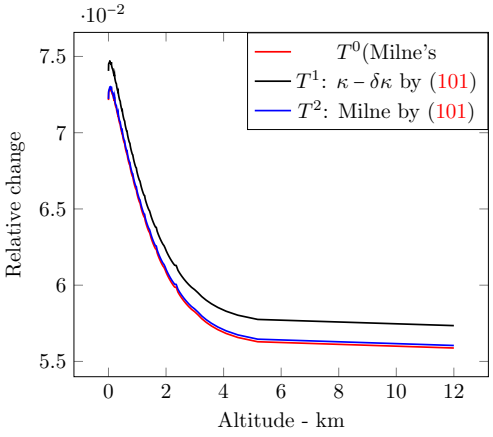

Figure 10: Temperature versus altitude. T^0 (in red) is the solution of Milne's problem with $\kappa_\nu = 1.225$ computed with (99)(100). T^1 (in black) is with $\kappa_\nu = 1.225 - 0.5\,\mathbf{1}_{\nu\in(0.2,0.3)}$ computed with (101). T^2 is computed with (101) with $\kappa = 1.225$ as if it was a non-constant function of ν (in blue).

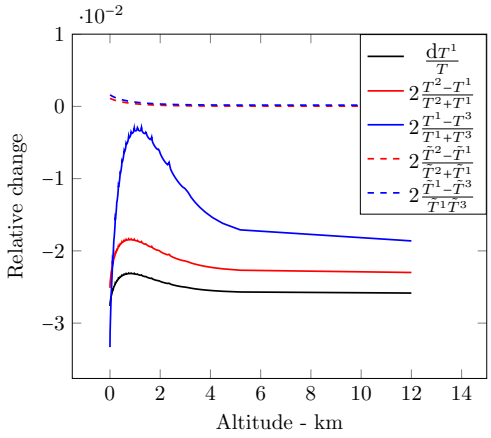

Figure 11: Relative temperature changes versus altitude, , computed with (101) or Automatic Differentiation (black), when $\kappa^1_\nu = 1.225 - 0.5\,\mathbf{1}_{\nu\in(0.2,0.3)}$, giving T^1, is changed to $\kappa^2_\nu = 1.225$, giving T^2. In red $2(T^2 - T^1)/(T^2 + T^1)$; in blue $2(T^1 - T^3)/(T^1 + T^3)$ with T^3 computed with $\kappa^3_\nu = 1.225 - 0.5\,\mathbf{1}_{\nu\in(0.1,0.4)}$ to account for a wider more transparent window of infrared absorption becoming narrower due to GHG. Finally the dashed curves with the corresponding colors are the same but with a more transparent window in the range $\tilde{\nu} \in (1., 1.2)$ and $\tilde{\nu} \in (1., 1.4)$.

7.3 Discussion on the reliability of the results

Greenhouse gases leading to a cooling of the atmosphere is counter intuitive. To check the codes we made a similar change of κ_ν but in a bigger range: $\kappa = 1 + 0.5\,\mathbf{1}_{(1,1.5)}$ where the precision should not be a

problem. Results are shown on figure 8: increasing κ in the range of sunlight leads to 0.5% increase on Earth temperature. The direct simulation of the change agrees with the calculus of variations. So the computer program is probably correct.

The change of κ_ν in a small frequency interval (0.2,0.3) could be beyond the numerical precision of the method and indeed figure 7 shows that the precisions may not be sufficient.

We make another remark relevant to precision:

Remark 6 *It is because the intersection of the Boltzmann curve for black body Earth with the Boltzmann curve for black body Sun is non zero (see figure 6) that there is an infrared re-emission due to sunlight on Earth.*

Proof : If the atmosphere is transparent to sunlight, $\kappa_\nu = 0,\ \forall \nu > 0.6$. Then $I_\nu|_{\tau=0,\mu>0} = \mu B_\nu(T_{Sun}),\ \forall \nu > 0.6$, and model (83) reduces to

$$\mu\partial_\tau I_\nu + \kappa_\nu(I_\nu - B_\nu) = 0,\ I_\nu|_{\tau=0,\mu>0} = \mu B_\nu(T_{Sun}),\ I_\nu|_{\tau=Z,\mu<0} = 0, \forall \nu < .6, \int_0^{.6} \kappa_\nu \left(B_\nu(T) - \frac{1}{2}\int_{-1}^{1} I_\nu\right) \mathrm{d}\nu = 0.$$

If we neglect $B_\nu(T_{Sun}),\ \nu < 0.6$, then there is nothing to drive the above system, so $I_\nu = 0,\ \nu < 0.6$. □

In our case $\nu_2 = 0.3$, $B_{\nu_2}(T_{Earth})|_{\tau=0} = 3.768\,10^{-4}$ and $B_{\nu_2}(T_{Sun})|_{\tau=0} = 3.569\,10^{-6}$; hence the interaction is very small. Is it the cause of lacks of numerical precision?

As a final check of the results of figure 9 and figure 11 we wrote an entirely different computer program to implement (91), in `C++`, linked to an Automatic Differentiation library: a technique based on operator overloading which gives the exact valued of derivatives of any variable in the program with respect to another variable, here the value of $\delta\kappa$ in the frequency range of GHG absorption. The program uses a uniform grid in τ, μ, by opposition to the `FreeFem++` program which uses a fairly uniform grid in the physical domain refined and adapted during computation to the Hessian of $\bar{I}$. It also produces a decrease of Earth temperature of the same magnitude!

All the numerical methods, implicit, finite element, uniform mesh (`C++`) and direct computation of the temperature difference or calculus of variations or automatic differentiation, give correct values for the temperatures versus altitude, but imprecise values to their derivative with respect to κ_ν; nevertheless all of them predict a decrease of temperature due to GHG when the absorption κ_ν increases in an infrared range (ν_1, ν_2) and when the range (ν_1, ν_2) is decreased.

8 Boundary layer near the Earth surface

Consider the Chandrasekhar equations with thermal diffusion: $\forall r, \mu, \eta \in (0, H) \times (-1, 1)^2$,

$$\mu\frac{\partial \bar{I}_\nu}{\partial r} + \frac{1-\mu^2}{R+r}\frac{\partial \bar{I}_\nu}{\partial \mu} + \kappa_\nu\rho\left(\bar{I}_\nu - B_\nu(T)\right) = 0, \tag{103}$$

$$-\frac{\kappa_T}{(R+r)^2}\left(\partial_r((R+r)^2\partial_r T) + \frac{1}{1-\eta^2}\partial_\eta^2 T\right) + \int_0^\infty \left(\rho\kappa_\nu(B_\nu(T) - \frac{1}{2}\int_{-1}^{1}\bar{I}_\nu \mathrm{d}\mu\right) d\nu = 0 \tag{104}$$

$$I_\nu(Z,\mu)|_{\mu<0} = 0, \quad I_\nu(0,\mu) = \mu Q_\nu, \quad \frac{\partial T}{\partial r}|_{0,Z} = 0 \tag{105}$$

where $\eta = \cos\theta$ and assume that $\kappa_T = \epsilon\kappa_0,\ \epsilon << 1$. Then it is likely that

$$T = T_0 + \epsilon T_1(\frac{r}{\sqrt{\epsilon}}, \mu),\ \ \bar{I}_\nu = I_0 + \epsilon I_1, \tag{106}$$

with $T_1(r,\mu) << 1$ when $r \to \infty$. This leads to the following cascade of equations

$$\mu\frac{\partial I_0}{\partial r} + \frac{1-\mu^2}{R+r}\frac{\partial I_0}{\partial \mu} + \kappa_\nu \rho\,(I_0 - B_\nu(T_0)) = 0, \quad B_\nu(T_0) - \frac{1}{2}\int_{-1}^{1} I_0 = 0, \tag{107}$$

$$\mu\frac{\partial I_1}{\partial r} + \frac{1-\eta^2}{R+r}\frac{\partial I_1}{\partial \mu} + \kappa_\nu \rho\,(I_1 - \partial_T B_\nu(T_0)T_1) = 0, \tag{108}$$

$$-\kappa_0\partial^2_{r'}T_1 + \int_0^\infty \left(\rho\kappa_\nu(\partial_T B_\nu(T_0)T_1 - \frac{1}{2}\int_{-1}^{1} I_1 \mathrm{d}\mu\right) = \frac{\kappa_0}{(R+r)^2}\left(\partial_r((R+r)^2\partial_r T_0) + \frac{\partial^2_\eta T_0}{1-\eta^2}\right) \tag{109}$$

with $r' = \sqrt{\frac{r}{\epsilon}}$. For clarity and without losing generality we assume R is large so as to reduces the above to

$$\mu\frac{\partial I_0}{\partial r} + \kappa_\nu \rho\,(I_0 - B_\nu(T_0)) = 0, \;\; B_\nu(T_0) - \frac{1}{4\pi}\int_{\mathbb{S}^2} I_0 = 0, \tag{110}$$

$$\mu\frac{\partial I_1}{\partial r} + \kappa_\nu \rho\,(I_1 - \partial_T B_\nu(T_0)T_1) = 0, \tag{111}$$

$$-\kappa_0\partial^2_{r'}T_1(r') + T_1(r')\int_0^\infty \rho\kappa_\nu \partial_T B_\nu(T_0)d\nu = \kappa_0\partial^2_r T_0 + \int_0^\infty \rho\kappa_\nu \frac{1}{2}\int_{-1}^{1} I_1 \mathrm{d}\mu d\nu. \tag{112}$$

The last line is also $-\partial^2_{r'}T_1 + bT_1 = c$, with $b = \frac{1}{\kappa_0}\int_0^\infty \rho\kappa_\nu\partial_T B_\nu(T_0)d\nu$ and $c = \partial^2_r T_0 + \int_0^\infty \frac{\rho\kappa_\nu}{2\kappa_0}\int_{-1}^{1} I_1 \mathrm{d}\mu d\nu$ Therefore

$$T(r) = T_0(r) + \epsilon\left(c + b\mathrm{e}^{-\sqrt{b}\frac{r}{\epsilon}}\right). \tag{113}$$

The conclusion is that there is no strong variation of the temperature $r \mapsto T(r)$ near the surface (r=0) due to thermal diffusion, but there is a strong variation of the gradient.

To connect with the next section we notice that (113) can be rewritten as:

$$\epsilon\frac{\partial(T-T_0)}{\partial r} + \sqrt{b}(T-T_0) = 0.$$

8.1 Boundary layer and Robin boundary condition

The temperature is a solution of an elliptic equation which requires a boundary condition on the entire boundary $\partial\Omega$ while the boundary condition for I needs to be given only on the incoming part of Σ_-.

Observe that (113) involves two temperatures $T_0(r)$ which could be expressed in term of I by the Stefan-Boltzmann law and a temperature $T(r)$ which represent the "observed temperature" near the boundary (which is unknown) and determined in term of non explicite constants. Such fact was already observed in nuclear reactor technology, where it leads for the diffusion approximation to a Robin boundary condition and is explained in [27] (p.199 eq. (8.13)).

Below, following [11] and [5] we propose a self contained derivation of this type of formula based on scaling analysis. Moreover for the sake of simplicity we consider the solutions I_ϵ of a ϵ dependent half space 0-flux (cf. section 5) Milne problem; one has the following

Proposition 4 *The family I_ϵ of solutions of the half space Milne Problem*

$$\epsilon I_\epsilon + \sqrt{\epsilon}\mu\partial_r I_\epsilon + I_\epsilon - \frac{1}{2}\int_{-1}^{1} I_\epsilon(r,\mu')d\mu' = 0\,, \;\; I(0,\mu)|_{\mu>0} = I(0), \tag{114}$$

$I(0)$ independent of μ, converges to the μ independent solution of the diffusion equation

$$\overline{I}_0 - \frac{1}{3}\partial^2_r\overline{I}_0 = 0 \text{ in } \mathbb{R}^+_r \tag{115}$$

with the Dirichlet boundary data $\overline{I}(0) = I(0)$, with a rate of convergence $O(\sqrt{\epsilon})$ in $L^2(\mathbb{R}^+\times(-1,1))$. However, the expression

$$I_0(r) - \sqrt{\epsilon}\mu\partial_r I_0(r) + \overline{\omega_1}\sqrt{\epsilon}\partial_r I_0(0) \tag{116}$$

provides an approximation of order ϵ in $L^\infty(\mathbb{R}^+\times(-1,1))$

One observes that I_ϵ is uniformly bounded in $L^\infty(\mathbb{R}^+ \times (-1,1))$ hence by standard estimates related to the diffusion approximation , it converges to a μ independent function $I_0(r)$ solution of (116) with $I_0(0) = I(0)$. Then one observes also that

$$\tilde{I}_\epsilon(r,\mu) = I_0(r) - \sqrt{\epsilon}\mu\partial_r I_0(r) \tag{117}$$

is a solution with an error of the order of $\sqrt{\epsilon}$ of the equation (114). This construction can be iterated giving a solution of any finite order of this equation. However, at $r = 0$ and $\mu > 0$ one has:

$$I(0,\mu) - \tilde{I}_\epsilon(0,\mu) = \sqrt{\epsilon}\mu\partial_r I_0(r) \tag{118}$$

and this estimation concerns a boundary layer of size $\sqrt{\epsilon}$ which can be only analyzed by the use of the zero flux solution $e(\tau,\mu)$ of the half space problem:

$$\mu\partial_r e + e - \frac{1}{2}\int_{-1}^{1} e(r,\mu')\mathrm{d}\mu' , \quad \text{for } \mu > 0 \quad e(0,\mu) = \mu . \tag{119}$$

Therefore one introduces the functions:

$$\begin{aligned} I_{\mathrm{rem}}(r,\mu) &= \left(\sqrt{\epsilon}\partial_r I_0(r)(e(\frac{r}{\sqrt{\epsilon}},\mu) - \overline{\omega_1}\right) + \sqrt{\epsilon}\overline{\omega_1}\partial_r I_0(r) \\ I_c(r,\mu) &= (I_0(r) - \sqrt{\epsilon}\mu\partial_r I_0(r,\mu)) - I_{\mathrm{rem}}(r,\mu). \end{aligned} \tag{120}$$

Constructed in such a way, $I_c(r,\mu)$ enjoys the following properties.

- It is a solution of the equation (114) with a remainder of order ϵ.
- For $r = 0$ and $\mu > 0$ one has $I_c(r,\mu) = I_0(0)$.
- I_{rem} is the sum of two terms $\sqrt{\epsilon}\overline{\omega_1}\partial_r I_0(r)$ and the boundary layer term:

$$BL_\epsilon(r,\mu) = \left(\sqrt{\epsilon}\partial_r I_0(r)(e(\frac{r}{\sqrt{\epsilon}},\mu) - \overline{\omega_1}\right). \tag{121}$$

According to the theorem 3 one has: $\sup_\mu |BL_\epsilon(r,\mu)| \le C^{-\alpha\frac{r}{\epsilon}}$.

As a consequence of these observations one has

$$I_\epsilon = (I_0(r) - \sqrt{\epsilon}\mu\partial_r I_0(r)) + \overline{\omega_1}\sqrt{\epsilon}\partial_r I_0(0) + O(\epsilon) \tag{122}$$

In an informal way the following can be derived:

Corollary 3 *Assume that the intensity of radiation I_ϵ of the above half-space Milne problem is coupled with the solution of a diffusion equation at the boundary of the domain by the Stefan-Boltzmann law; then the introduction of a Robin boundary condition of the type*

$$T_\epsilon(0) - 4\overline{\omega_1}\sqrt{\epsilon}\partial_r T_\epsilon(0) = T_0(0)\frac{T_0}{T_\epsilon} \tag{123}$$

in the diffusion approximation will improve it by an order of $\sqrt{\epsilon}$ to ϵ.

Proof : Starting from the relations

$$\sigma T_c^4(r) = \frac{1}{2}\int_{-1}^{1}(I_c)d\mu \quad \sigma T_0^4(r) = \frac{1}{2}\int_{-1}^{1}(I_0)d\mu \tag{124}$$

one deduces from (122) that

$$T^4(0) = T_0^4 + 4T_0^3\overline{\omega_1}\sqrt{\epsilon}\partial_r T_0 + O(\epsilon) \tag{125}$$

From which

$$T_\epsilon(0) - 4\overline{\omega_1}\sqrt{\epsilon}\partial_r T_\epsilon(0) = T_0(0)\frac{T_0}{T_\epsilon} \tag{126}$$

□

9 Conclusion

To summarize, we may say that radiative transfer is an old topic, studied by astronomers and nuclear scientists and more recently by climate modelers. Much of the ancient material can be discarded in view of the more powerful computer solutions. However, it turns out that for the simulation of the effect of sunlight on the atmosphere, the problem is numerically difficult, so that any mathematical and analytical properties gathered in the past are welcome.

Over the last fifty years the mathematical approach enjoyed stimulus from a huge range of applications, and the introduction of functional analysis and computing. However, one observes that there is still room for progress on the full model, in particular to make the hypothesis needed for proofs much more in agreement with the case considered in any kind of physics. As underlined above the equations (2),(3) leads to the following comments

- Concerning the time dependent equations, for sufficiently regular coefficients (κ, ρ and regular initial and boundary data), as it is expected, the problem has a unique well defined (for a finite time) solution, which can be extended on $[0, \infty)$ when the volumic sources $f = 0$ (cf. [25] for instance, for proofs and recent references). One of the main observation used in this contribution is the fact that an estimate of the type $0 < m(0) \leq T(\tau, 0) < M(0)$ remains valid for later time with $0 < m(t) < T < M(t)$.

- In ([25]) independent boundary conditions are assumed for I and T. It may be more realistic to include in the description some relation on the boundary. This would make use of the boundary layer analysis briefly described in the section (8).

- A more serious difficulty comes from the opacity $\kappa_\nu(\tau, T)$ which at variant with often made hypothesis (as in [24]) is possibly not regular (cf. [24]) and very often only vaguely known. At least two options have been taken in considering this issue. In one of the first contributions on the subject (cf [22]) it was assumed that, with no other hypothesis on the dependency on the frequency ν, the function $T \mapsto \kappa_\nu(T)$ was non increasing , while the function $T \mapsto \kappa_\nu(T)B_\nu(T)$ was non decreasing. Then some L^1 stability estimates lead to existence and uniqueness for the system.

  On the other hand the very popular (which leads to the Milne problem) grey model is based on a constant opacity with respect to ν. With such hypothesis several stability results have been obtained with no constraint on the regularity of the mapping $T \mapsto \kappa(T)$ (cf [1],[3],[4] and more recently [14]) for the treatment of the full problem with grey opacity.

- Under some convenient scaling hypothesis, in particular large opacity with respect to the size of the media one may approximate the dynamics by a diffusion equation known as the Rosseland approximation. Once again mathematical results are well advanced for the grey model and some of its variants and more sparse in the general case. Such approximation is very well adapted to describe "interior problems" like fusion by laser confinement. It does not seem (to the best of our knowledge) present in climatology. As a matter of fact, the height of the atmosphere being very small with respect to the Earth radius which seems to be considered is by itself a boundary layer. As sketched in the section 8.1 this issue is closely related to the improvement of the accuracy of the Rosseland approximation and also well developed for grey model. It is worth mentioning considering at the level of boundary layer the curvature of the atmosphere makes the problem even more subtle [29] and [28] for the Chandrasekhar equations (12).

Numerically, it is a mixed integro-differential problem for which a fixed point approach works quite well, and for which a convergence proof is available in the simpler case of Milne's.

Four methods of discretization have been tried. A finite element method with upwinding, a implicit method based on the integral form of the solution of the equation for the light intensity at given temperature, a finite difference implementation of the implicit method on a uniform mesh, with automatic differentiation, and finally an integral formulation for the temperature only. The second one is more precise but slower; the third is just for checking that the programs have no bugs, and the fourth one is the most trustworthy. So we may use it for validation . Convergence with respect to grid refinement is fairly fast.

All should be well and yet it is not. The difficulty lies in the very large scale differences between the infrared Earth radiations and the Sun light. This makes the evaluation of the tiny GHG effect difficult.

The present computations validate a decrease of Earth temperature due to CO_2 and other greenhouse gases responsible for a substantial change in the transmission coefficient κ_ν in the lower part of the infrared frequency range emitted by Earth seen as a black body at temperature $\sim 300K$; but it seems to be a cooling effect. Narrowing the infrared transparent window has also the same cooling effect. On the other hand, it gives a heating effect when the same changes on κ_ν occur in the lower frequency range of sunlight! If these numerically supported conclusions hold, then the radiative transfer equations, used with sunlight unaffected by the atmosphere, should not be presented as an explanation of the greenhouse effect using the infrared frequency range. However, the precision is such that the results should be believed only cautiously. Furthermore, let us keep in mind that the real problem of global warming is much more complex than just radiative transfer.

Acknowledgment

We thank Prof Guy Lucazeau for very valuable discussions, and Dr Benjamin Charnay for pointing to us the more important effect of GHG as a factor narrowing the infrared non-absorption range rather than increasing κ.

As the reader may want to improve these computations we will be happy to provide the computer codes on demand by email to the second author. Yet the `C++` program for the integral method described in paragraph 7.2 is given in appendix.

References

[1] C. Bardos: Problèmes aux limites pour les équations aux dérivées partielles du premier ordre à coefficients réels; théorèmes d'approximation; application à l'équation de transport. Ann. Sci. Ecole Norm. Sup. (4) (1970), 185-233.

[2] C. Bardos: Sur un théorème de perturbation d'équations d'évolution; application. C. R. Acad. Sci. Paris Sér. A-B 265 (1967), A169–A172.

[3] C. Bardos, F. Golse, and B. Perthame, The Rosseland approximation for the radiative transfer equations, Communications on Pure and Applied Mathematics, 40 (1987), pp. 691– 721.

[4] C. Bardos, F. Golse, B. Perthame, and R. Sentis, *The nonaccretive radiative transfer equations: existence of solutions and Rosseland approximation*, Journal of Functional Analysis, 77 (1988), pp. 434–460.

[5] C. Bardos, Santos, R. Sentis: Diffusion Approximation and computation of the critical size. Transactions of the American Mathematical Society Volume 284. Number 2. August 1984 pp. 617–649.

[6] Bensoussan, A., Lions, J.-L., Papanicolaou, G.C.: Boundary layers and homogenization of transport processes. Publ. Res. Inst. Math. Sci. 15(1), 53–157 (1979)

[7] K. M. Case, *Linear Transport Theory* Addison Wesley, Reading. 1967.

[8] S. Chandrasekhar, *Radiative Transfer*, Clarendon Press, Oxford, 1950.

[9] B. Charnay. ARIEL School `www.iap.fr/useriap/beaulieu/ARIEL/ARIEL-School2019-index.html`, Biarritz 2019.

[10] C. Cornet, Transfert radiatif dans une atmosphère tridimensionnelle : modélisation et applications en télédétection. Mémoire HdR. LAb. Optique atmosphérique, Univ. Lille. 2015.

[11] R. Dautray and J.L. Lions, *Mathematical Analysis and Numerical Methods for Science and Technology*, Tome 3 vol 9. Chap. 21 , Springer verlag, New-York, 2000.

[12] T.A. Davis, "Algorithm 832". ACM Transactions on Mathematical Software. 30 (2): 196–199, 2004.

[13] A. Fowler, *Mathematical Geoscience*, Springer Verlag, New-York 2011.

[14] M. Ghattassi, X Huo, and N. Masmoudi *On the diffusive limit of radiative heat transfert system I: Well prepared initial and boundary condition* ArXiv:2007.13209v [math.AP] 26 Jul. 2020.

[15] F. Golse, B. Perthame, R. Sentis: The nonaccretive radiative transfer equations: existence of solutions and Rosseland approximation. J. Funct. Anal. 77 (1988), no. 2, 434–460.

[16] E. Gros, Modélisation DART du transfert radiatif Terre-Atmosphère pour simuler les bilans radiatif, images de télédétection et mesures LIDAR des paysages terrestres. HAL Id: tel-00841795.

[17] D. Le Hardy, Y. Favennec, B. Rousseau and F. Hecht. Specular reflection treatment for the 3D radiative transfer equation solved with the discrete ordinates method. Journal of Computational Physics 334 (2017) 541–572.

[18] F. Hecht : New development in FreeFem++, J. Numer. Math., 20, pp. 251-265. (2012), (see also www.freefem.org.)

[19] G. Kanschat, E. Meinköhn, R. Rannacher, R. Wehrse (Eds) *Numerical Methods in Multidimensional Radiative Transfer*. Springer Verlag, Berlin (2000)

[20] H. Kapler and H. Hengler. Mathematics & Climate. SIAM publications. Philadelphia (2013).

[21] J. R. McCaa, M. Rothstein , B. E. Eaton, J. M. Rosinski, E. Kluzek and M. Vertenstein. User's Guide to the NCAR Community Atmosphere Model (CAM 3.0).

[22] B. Mercier, application of accretive operators theory to the radiative transfer equations, SIAM J. Math. Anal. Vol. 18, No. 2, March 1987.

[23] Michael F. Modest, *Radiative Heat transfer*, 3^{rd} ed., Academic Press, 2013.

[24] G. Pomraning *The equations of Radiation Hydrodynamics*, Pergamon Press, New-York, 1973.

[25] M. M. Porzio and O. Lopez-Pouso Application of accretive operators theory to evolutive combined conduction, convection and radiation Rev. Mat. Iberoamericana 20 (2004), 257–275.

[26] G. L. Stephens, D. O'Brien, P. J. Webster, P. Pilewski, S. Kato and Jui-lin Li. The albedo of Earth Reviews of Geophysics. Review article 10.1002/2014RG000449. (2014)

[27] Weinberg and Wigner *The Physical Theory if Neutrons Chain Reactors* , The University of Chicago Press, (1958).

[28] Wu, Lei : Boundary layer of transport equation with in-flow boundary. Arch. Ration. Mech. Anal. 235 (2020), no. 3, 2085–2169.

[29] Lei Wu, Yan Guo, Geometric Correction for Diffusive Expansion of Steady Neutron Transport Equation, Commun. Math. Phys. 336, 1473–1553 (2015)

10 Appendix

```
//
//  main.cpp
//  solve Milne problem and
//  solve multi-group for the same Milne for kappa=kappa2 constant (integration in nu)
//  and solve multi-group problem with  kappa=kappa2-dknu*(nu_1<nu<nu_2)
//
```

```
//  Created by Olivier Pironneau on 29/01/2021.
//

#include <iostream>
#include <fstream>
#include <cmath>

using namespace std;
#define sqr(x) (x*x)
const bool twoTemp=true; // if true, will measure the change due to change of kappa
const int n=3, MM=n*30; // nb points in tau
const int kmax=6+n;  // nb fixed point iterations
const double Z=1-exp(-12.); // max tau after change of var
const double SBsun = 4.036e-5;  // scaled sunlight power
const double Tsun = 1.126;  // scaled sun temperature
const double numax=20; // max frequency
const int jmax=150; // nb of points for integration in nu range
const double dnu0=numax/sqr(jmax);  // frequency minimal increment
const double dtt = 0.005; // integration step size in analytical formula
const int nt = 5; // min nb of integration step in anal formula
const double knu0=1.225; // absorption coeff and its GHS variation dknu
const double dknu=-0.5; // means knu0 and knu0+dknu0 are computed
const double nu01=0.2, nu02=0.3, nu03=0.1, nu04=0.4; // range of frequency for GHS absorption
const double pi = 4*atan(1.);
const double Bmilne=SBsun*sqr(sqr(Tsun*pi))/15;


double nu1, nu2;

double Inut[MM], Itk[MM], // mu integrals
        T[MM],  // Milner with knu0
        T1[MM], // T for knu0 + dknu*(nu1<nu<nu2)
        T2[MM], // Milner with knu0 by multi-group
        T3[MM]; // // T for knu0 + dknu*(nu3<nu<nu4)

double expint_E1(const double t, const double B=1){
    // if your compiler has it or if you can link to gosl you may adapt this function
    // it computes E1(t)*B
    const int K=8; // precision in the exponential integral function E1
    const double epst=1e-5, gamma =0.577215664901533; // special integration for log(t)
    if(t==0) return -1e12*B;
    double abst=fabs(t);
    if(abst<epst) return -abst*(gamma + log(abst)-1)*B;
    double ak=abst, somme=-gamma - log(abst)+ak;
    for(int k=2;k<K;k++){
        ak *= -abst*(k-1)/sqr(k);
        somme += ak;
    }
    return somme*B;
}
double Bsun(const double nu){ return SBsun*sqr(nu)*nu/(exp(nu/Tsun) -1);} // Boltzmann function

double BB(const double nu, const double T){ return sqr(nu)*nu/(exp(nu/T) -1);} // Boltzmann function

double intB(const double kappa, const double nu,const double tau,const double tmin,const double tmax){
    // returns the convolution t-integral of E1*B from t=tmin to tmax
    double aux=0;
    const double dt=fmin(dtt,nt/(tmax-tmin));
    for(double t=tmin;t<tmax;t+=dt){
        double baux = BB(nu,T[int((MM-1)*t/Z)]);
        if(kappa*(t-tau)!=0) aux += dt*kappa*expint_E1(kappa*fabs(tau-t),baux);
    }
    return aux;
}
```

```
int getT(const double kappa=knu0){ // return temperature by Kirchhof's law when kappa is constant
    for(int i=0;i<MM;i++){
        T[i]=sqrt(sqrt(15*Itk[i]/2/kappa))/pi;
    }
    return 0;
}

int getT1(){ // Kirchhof law when kappa is not constant
     for(int k=0;k<kmax; k++)
        for(int i=0;i<MM;i++){
            double Bik=Itk[i]/2;
            for(double nu=nu1; nu<nu2; nu+=dnu0) Bik -= BB(nu,T[i])*dknu*dnu0; // dknu correction
            T[i]=sqrt(sqrt(15*Bik/knu0))/pi;
    }
    return 0;
}

int getInu(const double kappa, const double nu){ // returns light intensity in frequency nu
    for(int i=0;i<MM;i++){
        double x=i*Z/(MM-1);
        Inut[i] = intB(kappa,nu,x,0,Z) + Bsun(nu)*(exp(-kappa*x)*(1-kappa*x)
                                                   + expint_E1(kappa*x,sqr(kappa*x)))/2;
    }
    return 0;
}

int getItTotal(){  // return total light intensity (only for milne with grey atmosphere)
    for(int k=0;k<kmax; k++){
      for(int i=0;i<MM;i++){
          double tau=i*Z/(MM-1);
          double aux=0;
        for(double t=0; t<Z;t+=dtt){
             if((t-tau)!=0) aux += dtt*expint_E1(knu0*fabs((tau-t)),Itk[int((MM-1)*t/Z)])/2;
        }
        T[i] = aux + Bmilne*(exp(-knu0*tau)*(1-knu0*tau) +
                             expint_E1(knu0*tau,sqr(knu0*tau)))/2;
      }
      for(int i=0;i<MM;i++)Itk[i]=T[i]*knu0; //T[] has been used as temporary memory
    }
    return 0;
}

int multiBlock()
{
    for(int i=0;i<MM;i++)  T[i]=0.07;  // initialize
     for(int k=0;k<kmax; k++){
        for(int i=0;i<MM;i++){ Itk[i]=0; Inut[i]=0;
        }
        double nu=0;
        for(int j=1; j<=jmax;j++){
            double dnu=(j+j-1)*dnu0;
            nu+=dnu;
            double kappa=knu0+dknu*(nu>nu1)*(nu<nu2); //kappa varies with nu
            for(int i=0;i<MM;i++) Itk[i]+=kappa*Inut[i]*dnu/2;
            getInu(kappa,nu);
            for(int i=0;i<MM;i++) Itk[i]+=kappa*Inut[i]*dnu/2;
        }
        getT1();
        std::cout << "k= "<<k<<" "<<T[2]<<" "<<T[MM-2]<<std::endl;
     }
     return 0;
}

int main(int argc, const char * argv[]) {
// computation with kappa variable and nu1,nu2
```

```
    std::cout<<"kappa variable\n iterations \t [T, dT] near earth and far near Z\n";
    nu1=nu01;  nu2=nu02;
    for(int i=0;i<MM;i++)  T[i]=0.07;  // initialize
    multiBlock();
    // computation with kappa variable and nu3,nu4
    nu1=nu03;  nu2=nu04;
    for(int i=0;i<MM;i++) T1[i]=T[i]; // store results in T1
        std::cout<<"kappa variable\n iterations \t [T, dT] near earth and far near Z\n";
        for(int i=0;i<MM;i++)  T[i]=0.07;  // initialize
        multiBlock();
        for(int i=0;i<MM;i++) T3[i]=T[i]; // store results in T3

// computation with kappa constant
    std::cout<<"\n kappa constant \n iterations \t [T, dT] near earth and far near Z\n";
    if(twoTemp){
        for(int i=0;i<MM;i++){  T[i]=0.07; } // initialize
        for(int k=0;k<kmax; k++){
            for(int i=0;i<MM;i++){ Itk[i]=0; Inut[i]=0; }
          double nu=0;
          for(int j=1; j<=jmax;j++){
                double dnu=(j+j-1)*dnu0;
                nu+=dnu;
              double kappa=knu0;  // kappa is constant
                for(int i=0;i<MM;i++) Itk[i]+=kappa*Inut[i]*dnu/2;
                getInu(kappa,nu);
                for(int i=0;i<MM;i++)Itk[i]+=kappa*Inut[i]*dnu/2;
          }
          getT();
          std::cout << "k= "<<k<<" "<<T[2]<<" "<<T[MM-2]<<std::endl; // store in T2
        }
    }
    for(int i=0;i<MM;i++) T2[i]=T[i];  // store results

    // Solve Milne problem to check
    for(int i=0;i<MM;i++)  Itk[i]=0.;  // initialize
    getItTotal();
    getT();  // results in T

    std::cout<<"\n tau\t [T] Milne \t [T1]:narrow [T2]:kappa cst [T3]:wide [T2-T1]/T  [T1-T3]/T \n ";
    ofstream  myfile = std::ofstream(
    "/Users/pironneau/Dropbox/aranger/TeX2021/climatthsCBOP/BardosPironneau/milneAD2.txt");
    for(int i=1;i<MM;i++){
       cout << -log(1-i*Z/(MM-1))<<"\t"<<T[i]<<"\t"<<T1[i]<<"\t"
                <<T2[i]<<"\t"<<T3[i]<<"\t"<<2*(T2[i]-T1[i])/(T2[i]+T1[i])
                <<"\t"<<2*(T1[i]-T3[i])/(T1[i]+T3[i])   <<std::endl;
       myfile   << -log(1-i*Z/(MM-1))<<"\t" // altitude
                <<T[i]<<"\t"         // T(Milner)
                <<T1[i]<<"\t"        // T(kappa+dknu) narrow frequency window
                <<T2[i]<<"\t"        // T(kappa) Milner by multigroup
                <<T3[i]<<"\t"        // T(kappa+dknu) wide frequency window
                <<2.*((T2[i]-T1[i]))/((T2[i]+T1[i]))<<"\t"  // (T(kappa)-T(kappa+dknu))/T
                <<2.*((T1[i]-T3[i]))/((T3[i]+T1[i]))<<"\t"  // (T(kappa)-T(kappa+dknu))/T
               <<std::endl;
    }
    return 0;
}
```